

CERN-EP-2022-111

01 June 2022

Closing in on critical net-baryon fluctuations at LHC energies: cumulants up to third order in Pb–Pb collisions

ALICE Collaboration*

Abstract

Fluctuation measurements are important sources of information on the mechanism of particle production at LHC energies. This article reports the first experimental results on third-order cumulants of the net-proton distributions in Pb–Pb collisions at a center-of-mass energy $\sqrt{s_{\text{NN}}} = 5.02$ TeV recorded by the ALICE detector. The results on the second-order cumulants of net-proton distributions at $\sqrt{s_{\text{NN}}} = 2.76$ and 5.02 TeV are also discussed in view of effects due to the global and local baryon number conservation. The results demonstrate the presence of long-range rapidity correlations between protons and antiprotons. Such correlations originate from the early phase of the collision. The experimental results are compared with HIJING and EPOS model calculations, and the dependence of the fluctuation measurements on the phase-space coverage is examined in the context of lattice quantum chromodynamics (LQCD) and hadron resonance gas (HRG) model estimations. The measured third-order cumulants are consistent with zero within experimental uncertainties of about 4% and are described well by LQCD and HRG predictions.

*See Appendix A for the list of collaboration members

1 Introduction

Predictions based on the theory of the strong interaction, QCD, imply that, at sufficiently high energy densities, nuclear matter transforms into a state called quark–gluon plasma (QGP) [1, 2], where chiral symmetry is restored and quarks and gluons are deconfined. Ultrarelativistic heavy-ion collisions are ideal environments to study the phase diagram of strongly interacting matter and the physics of the QGP state as a function of temperature (T) and baryon chemical potential (μ_B). While the QCD phase diagram is largely unknown for $\mu_B > 450$ MeV, the region below that value down to $\mu_B = 0$ has been well explored theoretically [2, 3] and experimentally [4]. In that region, the chiral phase transition is most likely a continuous crossover with pseudo-critical temperature $T_{pc} \approx 157$ MeV at $\mu_B = 0$ [5, 6]. Near $\mu_B = 0$ the properties of the QCD phase transition depend on the number of quark flavors and their masses. For vanishing masses of the light quarks (u,d) the transition is of second order and belongs to the universality class of three-dimensional O(4)-symmetric spin models [7]. The small u,d quark masses of order of 1% of the constituent quark masses constitute a small but explicit breaking of chiral symmetry. For these small physical quark masses LQCD indicates that the transition turns into a smooth crossover. To date, there is no experimental confirmation of the crossover nature of the transition. Nevertheless, the smallness of the physical quark masses may leave traces of critical behavior also for a crossover transition. Therefore, a significant effort at the RHIC and LHC colliders is concentrated on quantifying the nature of the phase transition in the small μ_B region.

For large μ_B the phase diagram may exhibit a “critical endpoint (CEP)”. The search for the CEP is one of the main physics goals of the beam energy scan programs at RHIC [8, 9], at the CERN SPS [10], and at FAIR [11].

Recent LQCD [12–14] calculations of chiral susceptibilities, derivatives of the chiral condensate with respect to quark masses, exhibit for small quark masses a clear peak at T_{pc} , consistent with the chemical freeze-out temperature extracted by the analysis of hadron multiplicities [4, 15] measured in central Pb–Pb collisions by the ALICE experiment. This suggests that the chemical freeze-out occurs very close to the chiral phase transition at LHC energies. Critical signals associated with this phenomenon can be linked with long-range correlations and increasing multiplicity fluctuations due to the existence of the massless modes of the second-order phase transition [16, 17]. In particular, the fluctuations of the conserved charges are very sensitive probes for the equation of state and can be directly related to the thermodynamic susceptibilities, which are calculable in the framework of LQCD. The quark-number susceptibilities are defined as the derivatives of the reduced QCD pressure (P/T^4) with respect to the reduced chemical potentials ($\hat{\mu} = \mu/T$) of the conserved charges

$$\chi_{klmn}^{B,S,Q,C} = \frac{\partial^{(k+l+m+n)}(P(\hat{\mu}_B, \hat{\mu}_S, \hat{\mu}_Q, \hat{\mu}_C)/T^4)}{\partial \hat{\mu}_B^k \partial \hat{\mu}_S^l \partial \hat{\mu}_Q^m \partial \hat{\mu}_C^n} \Big|_{\hat{\mu}=0}. \quad (1)$$

Here the relevant conserved charges, represented by the chemical potentials, are the electric charge Q , the baryon number B , the strangeness S , and the charm C . These susceptibilities are studied experimentally in terms of the ratios of the cumulants¹ of net-charge distributions [19]. Here and in the following, net-charge distribution stands for the difference between the distributions of positively and negatively charged particles, where “charge” refers to any additive quantum number. Signs of criticality due to the proximity of the chiral crossover transition to a second-order transition are expected to show up starting only with the sixth-order cumulants of net-charge distributions [16, 20]. Measuring conserved charge fluctuations in ultrarelativistic nuclear collisions is a challenging task, see Ref. [8] for a recent review. In addition to possible critical fluctuations due to the proximity of a CEP or O(N) criticality, there are several other dynamical signals, such as correlations due to baryon number conservation [21–23],

¹The cumulants, κ_n , of net-baryon number, $\Delta N_B = N_B - \bar{N}_B$, are defined as the coefficients in the Maclaurin series of the logarithm of the characteristic function of ΔN_B [18].

volume fluctuations [18], thermal blurring [24], resonance decays [23, 25], initial-state fluctuations [26], baryon annihilation [27], “excluded volume” effects [23], etc., which could overshadow the dynamical fluctuations of interest.

The article is organized as follows. In Section 2, details are given about the ALICE detector, the data set and the analysis procedure, such as event and track selection criteria, particle identification and the efficiency correction technique. In Section 3, results on second-order cumulants of net-pion and net-kaon distributions are presented to demonstrate the influence of resonance decays on the measured cumulants. The main results are contained in the second- and third-order cumulants of net-proton distributions and compared to theoretical expectations. The article concludes, in Section 4, with a discussion on how the present results fit into the general strategy to get information on possible critical behavior near the QCD phase boundary and with an outline of the next steps.

2 Experimental setup and data analysis

The measurements presented in this article are based on about 13 and 78 million minimum bias Pb–Pb collisions at $\sqrt{s_{\text{NN}}} = 2.76$ and 5.02 TeV recorded with the ALICE detector [28, 29] in the years 2010 and 2015, respectively. Note that the running conditions have changed significantly in 2015. The details presented in this article refer only to the analysis of 2015 data (see Refs. [30, 31] for 2010). The minimum-bias trigger condition is defined by requiring a coincidence of hits in both V0 detectors [32] located on either side of the nominal interaction point along the beam direction and covering the pseudorapidity intervals $2.8 < \eta < 5.1$ and $-3.7 < \eta < -1.7$. The definition of the centrality [33] is based on the signal amplitudes measured in the V0 detectors, which are related to the collision geometry and the number of participating nucleons through a Monte Carlo (MC) simulation based on a Glauber model [34, 35]. Beyond event characterization, the main sub-detectors used in the analysis are the Time Projection Chamber (TPC) [36] for tracking and particle identification (PID), using the specific energy loss dE/dx , and the Inner Tracking System (ITS) [37, 38] for tracking and vertex determination.

Event and track selection criteria were applied to ensure optimal PID performance via dE/dx measurement and momentum (p) resolution, as well as good track quality. The V0 [32] and the Zero Degree Calorimeter [39] timing information was used to reject background due to beam–gas interactions and parasitic beam–beam interactions. Along the beam direction, events occurring within ± 0.15 cm, where tracking is affected by the central membrane of the TPC, and outside ± 7 cm of the nominal interaction point were discarded to keep detection efficiency uniform as a function of event vertex position. This corresponds to 24% of the total events.

The analysis uses tracks of charged particles reconstructed using the ITS and the TPC in the pseudorapidity range of $|\eta| < 0.8$ and with full azimuthal acceptance. Due to the different gas mixture, higher interaction rates, and larger multiplicities in 2015, the TPC performance was affected by local space-charge distortions caused by the accumulation of space charge originating from the gaps between adjacent readout chambers [40]. Although these distortions are corrected on average during reconstruction, their fluctuations caused a significant mismatch between the TPC and ITS tracks. They affected all events detected within a time interval of about 0.5 seconds after a collision, corresponding to the full drift time of ions from the amplification region in the TPC readout chambers to the central electrode. Collisions within such time intervals were discarded using the event interaction time (timestamp), when in addition the mean matching efficiency between the TPC and ITS for all tracks was less than 88%. The nominal TPC–ITS track matching efficiency is narrowly peaked at 90.5%. By applying this condition about 7% of all events are rejected. Tracks were accepted if their χ^2 value per space point from the track fit is less than 3.5. To improve the dE/dx resolution and reduce the contributions from track splitting², two additional track selection criteria were applied. The number of clusters used for the dE/dx calcula-

²Track splitting occurs when a track is reconstructed as two separate tracks due to poor dE/dx resolution.

tion³ was set to more than 70, and short tracks crossing less than 80 out of a maximum of 159 pad rows were excluded from the analysis. These criteria address both tracks crossing chamber boundaries and split tracks, both leading to a deterioration of the dE/dx measurement. To suppress contributions from particles from weak decays and interactions in the detector material, the distance of closest approach (DCA) of the extrapolated track to the primary vertex position was required to be less than 1 cm along the beam direction, while in the transverse plane a transverse momentum (p_T) dependent DCA selection of less than $(0.018 \text{ cm} + 0.035 p_T^{-1.01})$ with p_T in GeV/c was applied to account for the p_T dependence of the DCA resolution [41]. In addition, daughter tracks from reconstructed secondary weak-decay kink topologies were discarded.

In 2015, the ALICE TPC was operated at interaction rates up to 8 kHz during Pb–Pb collisions. These high interaction rates resulted in a possible pile-up of several interactions during the 90 μs drift time. The fraction of pile-up events that occur within a few cm of the primary vertex, the so-called in-bunch pile-up, is less than 1% of the entire data set. Therefore, in-bunch pile-up has a negligible impact on the results. Moreover, in-bunch pile-up events were further suppressed thanks to the high-precision vertexing capabilities of the ITS. Even slightly displaced multiple vertices originating from interactions within the same bunch crossing can be discriminated. The much more frequent out-of-bunch pile-up events occur anytime during the drift time of the TPC, i.e., they are distributed equally along the time direction within the TPC and cannot be suppressed by reconstructed secondary vertices in the ITS. They lead to a significant deterioration in the measurements of the dE/dx of the triggered event caused by the baseline fluctuations in the TPC [40]. These pile-up events affect about 20% of the data collected in 2015 and are negligible for 2010. The resulting bias in the measured dE/dx is corrected to restore optimal PID performance and to avoid the need to discard events with pile-up [40].

Protons are identified by their dE/dx in the TPC and its known momentum dependence. To overcome the misidentification problem caused by overlapping dE/dx distributions for different particles, for instance at the crossings of kaons (K) and protons (p) or pions (π) and protons, a novel experimental technique, the Identity Method (IM) [42–44] was used. With this method, weights, which are obtained from the fits of dE/dx distributions, are assigned to each track reflecting the probability of a particle having a specific identity. Thereby all tracks can be kept without applying any selection on the PID variable and no second detector needs to be employed to identify the (anti)protons. In the present analysis, particles in the momentum range 0.6–2.0 GeV/c were retained. With particle identification based solely on the dE/dx measurements in the TPC, the efficiencies are independent of momentum in the selected range, and as high as about 91% for protons and about 83% for antiprotons. The difference of 8% is due to the absorption of antiprotons in the detector material. Both proton and antiproton detection efficiencies are nearly independent of collision centrality and are uniform within the kinematic acceptance used in this analysis. The cumulants of the net-proton distribution are reconstructed using the IM as well. Further details on the application of the IM to ALICE data are discussed in Ref. [31]. In Ref. [30], the method used here was applied to the analysis of second-order cumulants of net protons in Pb–Pb collisions at $\sqrt{s_{\text{NN}}} = 2.76 \text{ TeV}$. The current analysis closely follows what is described there.

Understanding and controlling the particle detection efficiency is one of the major technical challenges in the measurement of higher-order cumulants, since the efficiency enters into the analytical formula of the correction with the corresponding higher power [45–47]. This affects both statistical and systematic uncertainties of the corrected data. Note that the efficiency correction approximately doubles the statistical uncertainties, as also noted in Ref. [48]. The efficiency correction for the cumulants is performed by using proton and antiproton efficiencies in analytic formulas derived in Refs. [45–47] assuming efficiency losses governed by the binomial statistics (binomial efficiency loss). In order to ensure that this

³Clusters that are very close to the TPC readout chamber boundaries [40] or are from overlapping tracks are not considered in the calculation of dE/dx . Therefore, the number of clusters used to calculate dE/dx may differ from the number of clusters used for track selection. This quantity is particularly important for the dE/dx resolution.

assumption is fulfilled, the ALICE detector response [29] was studied in detail with a full MC simulation using the HIJING event generator and the GEANT4 [49] transport software. The response of the TPC detector for the kinematic range used in this analysis is illustrated in the left panel of Fig. 1 as a correlation between the reconstructed (N_p^{rec}) and the generated (N_p^{gen}) number of protons, where the reconstructed protons are those detected in the active area of the detector, as well as satisfying the event and track quality criteria. The event and track selection plays a significant role in the shape of the TPC detector response. For example, as discussed above, they can reduce the contributions from track splitting, which causes correlated dE/dx measurements, and thus a deviation from a binomial detector response.

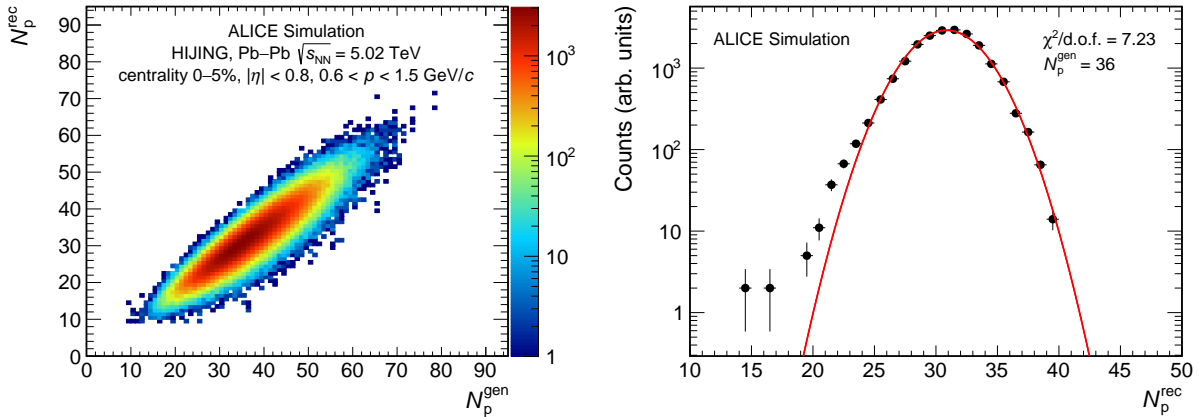


Figure 1: (Left) Correlation between the reconstructed (N_p^{rec}) and the generated (N_p^{gen}) number of protons for the most central Pb–Pb collisions simulated using the HIJING model [50]. (Right) Distribution of reconstructed proton number for a fixed value of $N_p^{\text{gen}} = 36$, where the fit demonstrates the deviation from a binomial efficiency loss.

After detailed study and optimization of the event and track selection, only a slight deviation from the binomial loss is observed, as shown in the right panel of Fig. 1. A MC verification test was performed to estimate the impact of this deviation in the final results on the net-proton cumulant measurements. In this MC closure test, particles are generated, including certain correlations such as the effect of baryon number conservation, and reconstructed after they have passed through the detector simulated with GEANT4. Then the efficiency correction is applied, and the generated and corrected observables are compared. The comparison is shown in Fig. 2 for the second- and third-order cumulant ratios of the net-proton distribution. The efficiency-corrected results obtained from the MC reconstructed data are in agreement with the results obtained from the MC generated data. Note that the uncorrected results, also in Fig. 6, deviate from the Skellam baseline, which is set at zero, because the net-proton number is nonzero due to antiproton absorption in the detector material and, to a smaller degree, by a proton knock-out contribution. Therefore, the final results depend crucially on a very accurate determination of the proton and antiproton efficiencies.

The statistical uncertainties assigned to the reconstructed cumulants were determined using the subsample method. To this end, the data set was subdivided into n random subsamples. The distribution of the cumulants from these subsamples yields the statistical uncertainty as described in Ref. [31]. The fits to the measured dE/dx distributions, which are the only inputs to the IM, are the dominant source of systematic uncertainty in the ratios of the cumulants, for both second and third order. The observed maximum deviation between fit variations [31] is 0.6% and 0.8% for the normalized second-order cumulants within the momentum intervals of 0.6–1.5 GeV/c and 0.6–2.0 GeV/c , respectively, and 4% for the ratio of third- to second-order cumulants in the momentum interval 0.6–1.5 GeV/c . The impact of possible imperfections in the dE/dx correction procedure mentioned above is also included in this systematic uncertainty estimate by analyzing the data retaining different fractions of events containing pile-up. The uncertainties associated with the detection efficiencies of the (anti)protons are also investigated by varying the detection efficiencies by an amount of $\pm 2\%$ for protons and antiprotons separately. The resulting

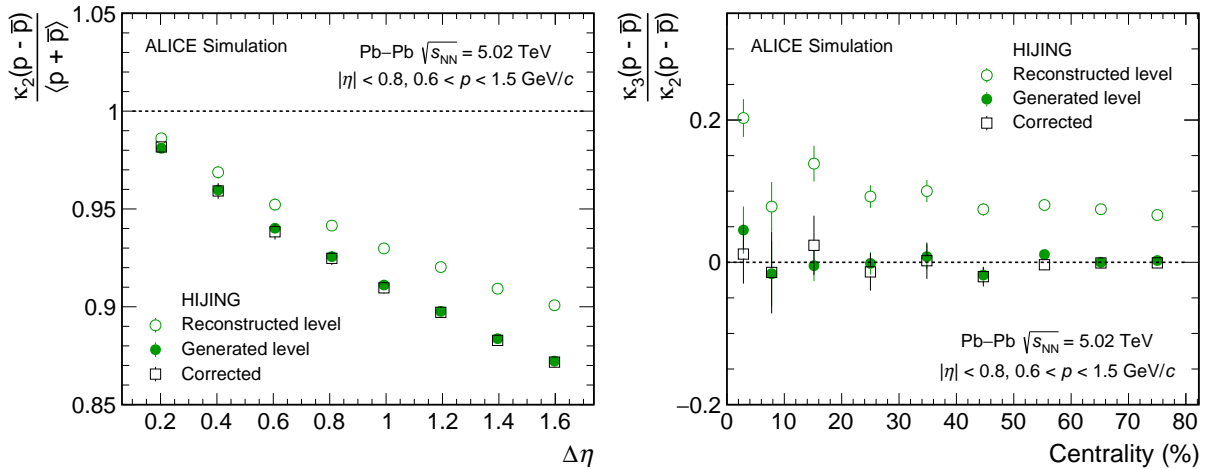


Figure 2: HIJING model [50] based calculations of the normalized second-order cumulants of net protons as a function of pseudorapidity window ($\Delta\eta$) (left) and ratio of third- to second-order cumulants (right) of net protons as a function of collision centrality at $\sqrt{s_{\text{NN}}} = 5.02$ TeV. The results at the generated and reconstructed level are shown by the green closed and open circles, respectively. The error bars represent statistical uncertainties. The results after efficiency correction assuming binomial efficiency losses [45–47] are shown by black open squares.

systematic variation is less than 0.2% and 1.5% for the second- and third-order cumulants, respectively. Other sources of systematic uncertainty are estimated by varying the event and track selection criteria, resulting in a maximum uncertainty of less than 1%. The final total systematic uncertainty is obtained by adding in quadrature the individual maximum systematic deviations from these three groups of independent contributions. For the third-order cumulants, it varies between less than 0.5% for the most peripheral collisions and a maximum of 3% for the most central collisions for the pseudorapidity interval of $\Delta\eta = 1.6$.

3 Results

As potential candidates for conservation of electric charge and strangeness, results are reported for the pseudorapidity interval dependence of the second-order cumulants of net-pions and net-kaons produced in central Pb–Pb collisions.

The observations in these channels are quite striking because they shed light on resonance decay contributions to fluctuations in Pb–Pb collisions at the LHC. Figure 3 shows the pseudorapidity interval dependence of the normalized second-order cumulants of net-pions and net-kaons compared with the results from HIJING [50] with and without resonance contributions. A significant effect of resonances, e.g., $\rho \rightarrow \pi^+\pi^-$ and $\phi \rightarrow K^+K^-$, is clearly visible in both cases. In fact, the decay of resonances into oppositely charged pion or kaon pairs drastically reduces the fluctuations and dominates the second-order cumulants of the respective net distributions. Therefore, to study the genuine electric charge and strangeness fluctuations, first a quantitative understanding of the resonance contributions is essential. On the other hand, there are no resonances that decay into $p\bar{p}$ with a sizeable branching ratio, therefore net-proton fluctuations are not obscured by this effect. It has been argued in the literature [51] that net-proton fluctuations are good proxies for net-baryon fluctuations, in particular for $\sqrt{s_{\text{NN}}} > 10$ GeV. Also, total electric-charge conservation is expected to have a negligible impact on the net-proton fluctuation measurements, since the electric charge is mostly carried by the charged pions, which are the most abundant species at LHC energies. The statistically independent Poisson limit for net-baryon distributions is the Skellam distribution, which is defined as the probability distribution of the difference of two random variables, each generated from statistically independent Poisson distributions [52, 53]. For net protons,

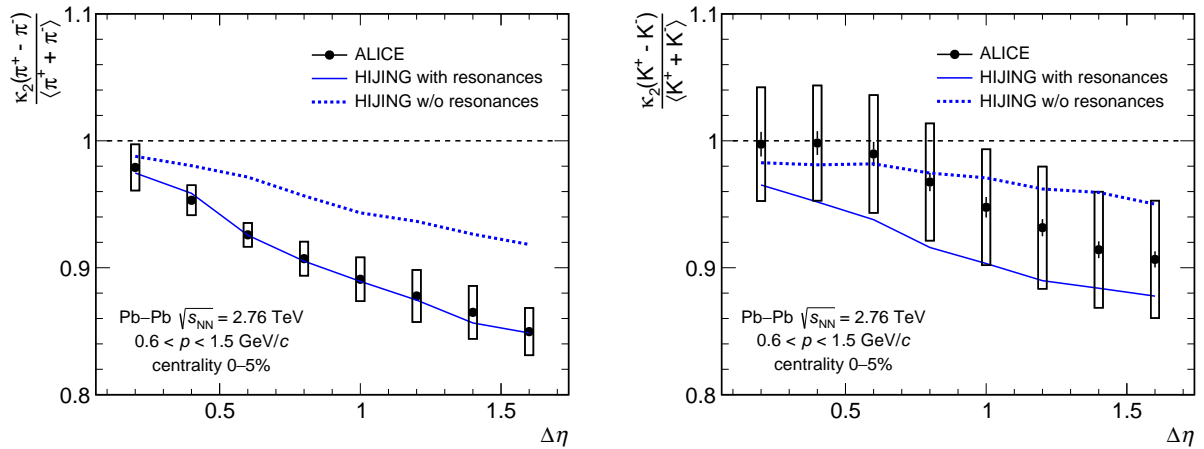


Figure 3: Pseudorapidity interval dependence of the second-order cumulants of net-pions (left) and net-kaons (right) normalized to the means (see text). The ALICE data are shown as solid black circles while the blue solid and dashed lines indicate the results from HIJING [50] model calculations with and without resonance contributions, respectively. The error bars represent statistical uncertainties and the boxes around the data points represent the total systematic uncertainties.

the n th-order cumulants of the Skellam distribution are given by

$$\kappa_n^{\text{Skellam}}(p - \bar{p}) = \langle p \rangle + (-1)^n \langle \bar{p} \rangle, \quad (2)$$

where $\langle p \rangle$ and $\langle \bar{p} \rangle$ are the mean values of the proton and antiproton multiplicity distributions, respectively. That means that even-order cumulants of the Skellam distribution of the net protons are just the sum of the mean numbers of protons and antiprotons. At LHC energies, these numbers are equal within 1% [54], and therefore the normalized cumulants of the Skellam distribution with respect to its second-order cumulant are zero for odd cumulants and unity for even cumulants. At T_{pc} [5, 6], both the predictions based on LQCD and the HRG [4] model agree with the Skellam baseline up to the third-order cumulants of the net protons, reflecting independent Poissonian fluctuations. The LQCD prediction [55], including the effect of dynamical quarks, shows a significant deviation from the Skellam baseline for the fourth- and higher-order cumulants, while the standard HRG does not contain such effects and deviations from the Skellam baseline are only due to baryon number conservation [56]. Fluctuations of conserved charges are meaningful only within a limited phase space. They vanish in the full phase space, in order to obey the conservation laws, and asymptotically approach the Poisson limit for very small acceptance, where dynamical correlations are suppressed [45]. Therefore, the fluctuations of net-baryons are studied in the framework of the Grand Canonical Ensemble, where the net-baryon number is conserved only on average. Accordingly, the analysis is performed differentially as a function of the collision centrality, the pseudorapidity interval, $\Delta\eta = 0.2$ to 1.6 , and for two different momentum ranges, 0.6 – 1.5 GeV/c and 0.6 – 2.0 GeV/c . It should be noted that the determination of centrality and the net-proton analysis are based on measurements in different pseudorapidity intervals to avoid trivial effects due to autocorrelations [18].

Figure 4 shows the measured centrality and pseudorapidity dependence of the normalized second-order cumulants of the net protons in Pb–Pb collisions for the two collision energies. The 5.02 TeV data appear to be somewhat lower, however the two data sets agree within systematic uncertainties. It should be noted that the systematic uncertainties exhibit a large degree of correlation from bin to bin, but between the two collision energies are essentially uncorrelated due to the different running conditions (collision rate, gas mixture and space charge distortions in the TPC, etc.). The normalized second-order cumulants are independent of collision centrality and are reduced by about 5% from the Skellam baseline for the $\Delta\eta = 1.6$ interval (left panel). As a function of the width of the $\Delta\eta$ interval, the fluctuations

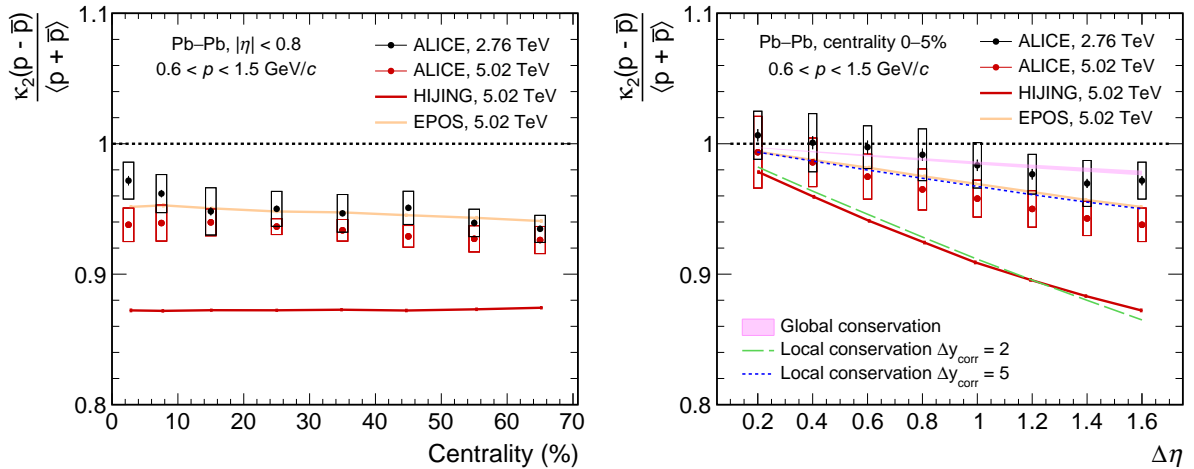


Figure 4: (Color online) Centrality (left) and pseudorapidity interval (right) dependence of the normalized second-order cumulants of net protons. The ALICE data are shown by black and red markers for $\sqrt{s_{\text{NN}}} = 2.76$ TeV and 5.02 TeV, respectively, while the colored shaded areas indicate the results from HIJING [50] and EPOS [57] model calculations at $\sqrt{s_{\text{NN}}} = 5.02$ TeV. The Skellam baseline is shown by the horizontal dashed black line. In the right panel the expectation from global baryon number conservation is shown as a pink band and the dashed colored lines represent the predictions of the model with local baryon number conservation [22].

are increasingly reduced. Due to the increasing relevance of baryon number conservation with larger acceptance, this is expected. For the narrowest interval, statistically independent Poissonian fluctuations are observed. The results are also compared to results from HIJING [50] and EPOS [57] model calculations at $\sqrt{s_{\text{NN}}} = 5.02$ TeV. HIJING treats nucleus–nucleus collisions as an independent superposition of nucleon–nucleon interactions and does not include phenomena such as equilibrium and collectivity. While in HIJING the hadronization is based on the Lund string fragmentation scheme, EPOS (version 1.99, tuned to LHC data) distinguishes between string segments in a collectively behaving central part (“core”) with high energy density and those in a peripheral part (“corona”) with lower energy density, more like in pp or p–A collisions.

It is noteworthy that the proton to antiproton ratio is above unity in both models with a significance of more than 3 sigma: 1.025 ± 0.004 and 1.008 ± 0.002 for EPOS and HIJING, respectively; the value measured by ALICE in Pb–Pb collisions at $\sqrt{s_{\text{NN}}} = 2.76$ TeV agrees with unity within experimental uncertainties of a few percent [54]. This implies that the volume fluctuations for the second- and third-order cumulants are not negligible for the model calculations [18].

Both model calculations show second-order fluctuations independent of centrality, as do the experimental data. The results from the EPOS calculations agree within the uncertainties with the data both in terms of the centrality and the $\Delta\eta$ dependencies. The HIJING model results exhibit a 12% suppression compared to Poissonian fluctuations for the widest $\Delta\eta$ interval and are significantly below the data. This is also apparent in the dependence on the width of the $\Delta\eta$ interval (right panel of Fig. 4). The dependence on acceptance, and specifically the discrepancy between the HIJING results and the data, is examined in view of global vs local baryon number conservation modelled in Refs. [18, 22, 30, 56] using a canonical statistical model. The right panel of Fig. 4 shows the results for different widths of the correlation interval, ranging from global baryon number conservation to short-range correlations. As expected, measurements and model calculations converge to the Skellam baseline in the limit of very small acceptance. As already noted in Ref. [30], the data from ALICE indicate long-range rapidity correlations ($\Delta y_{\text{corr}} > 5$) between protons and antiprotons, therefore originating from the early phase of the collision [58]. Here $\Delta y_{\text{corr}}/2$ is defined as the correlation length between protons and antiprotons in rapidity [22], so that $\Delta y_{\text{corr}} = 5$ means that protons are correlated with antiprotons within 2.5 rapidity units

into either direction.

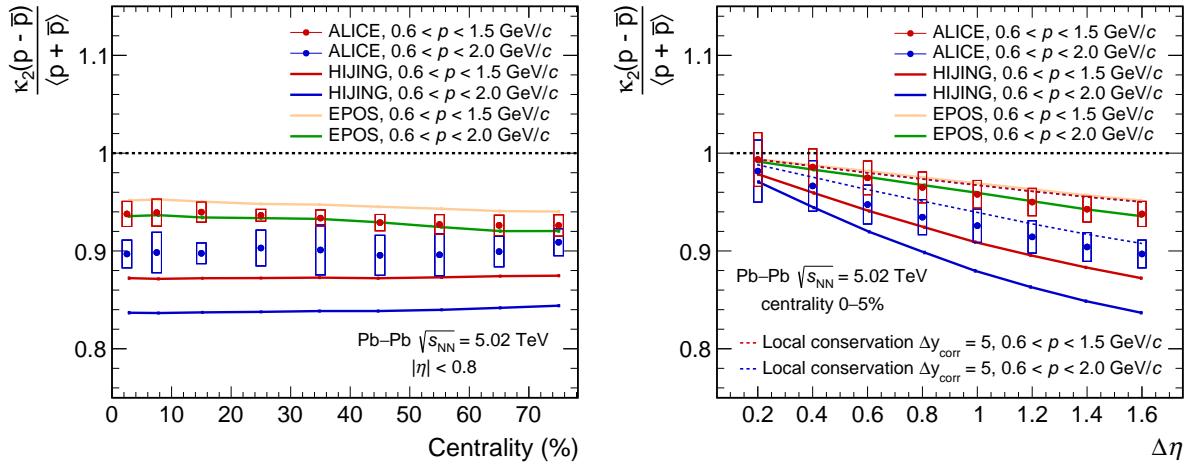


Figure 5: (Color online) Centrality (left) and pseudorapidity interval (right) dependence of the normalized second-order cumulants of net protons for $\sqrt{s_{\text{NN}}} = 5.02$ TeV and two momentum intervals for the protons. The ALICE data are shown by red and blue markers for $0.6 < p < 1.5$ GeV/c and $0.6 < p < 2.0$ GeV/c, respectively. The colored shaded areas indicate the results from the HIJING [50] and EPOS [57] model calculations. In the right panel, in addition, the dashed colored lines represent the predictions from the model with local baryon number conservation with $\Delta y_{\text{corr}} = 5$ [22].

The HIJING model calculations reflect a much smaller correlation length ($\Delta y_{\text{corr}} = 2$) than the EPOS model ($\Delta y_{\text{corr}} = 5$) and the ALICE data. This is likely due to the formation of baryons in string breaking in the underlying Lund string model [59]. This sensitivity to the range of proton–antiproton correlations is further studied by enlarging the momentum acceptance for the $\sqrt{s_{\text{NN}}} = 5.02$ TeV data. The resulting normalized second-order cumulants are shown in Fig. 5 for the momentum intervals 0.6–1.5 GeV/c and 0.6–2.0 GeV/c. Using the wider momentum interval the number of protons and antiprotons roughly doubles. While there is again no change with the collision centrality, the larger acceptance leads to a larger suppression of fluctuations for the wider momentum range. For the largest $\Delta\eta$ interval, the suppression amounts to an additional 4%. All calculations reflect the reduction in the fluctuations. However, while the magnitude is properly reproduced by the canonical statistical model predictions with a long correlation length [22], it can be noted that the suppression due to increased acceptance is somewhat weaker in the EPOS results. The HIJING calculations properly track the absolute reduction in fluctuations, but fall significantly below the data in absolute amount.

Figure 6 shows the centrality and pseudorapidity dependence of the ratio of third- to second-order cumulants of net protons at $\sqrt{s_{\text{NN}}} = 5.02$ TeV before and after the efficiency correction. After efficiency correction, the data agree with the zero baseline within the experimental uncertainties, which is consistent with expectations from the HRG model. The experimentally achieved overall precision is better than 4% for the most central collisions and much smaller for more peripheral collisions. Note that in the HRG model all odd cumulants vanish at LHC energy, where the number of baryons and antibaryons agree. The odd cumulants vanish under these conditions also if baryon number conservation is included, see Refs. [56, 60]. Also in LQCD [61] the odd cumulants vanish.

In Fig. 7, the third-order cumulant measurements are also compared with HIJING and EPOS model calculation results. Both models include baryon number conservation but, as mentioned above, the net-proton number is positive within the current experimental acceptance. Therefore, the resulting third-order cumulants for all centrality and pseudorapidity difference intervals shift toward positive values and are affected by the volume fluctuations [18] visible in the 10–20% centrality interval, where the centrality range doubles (left panel). The consistency of the experimental results of the third- to second-order

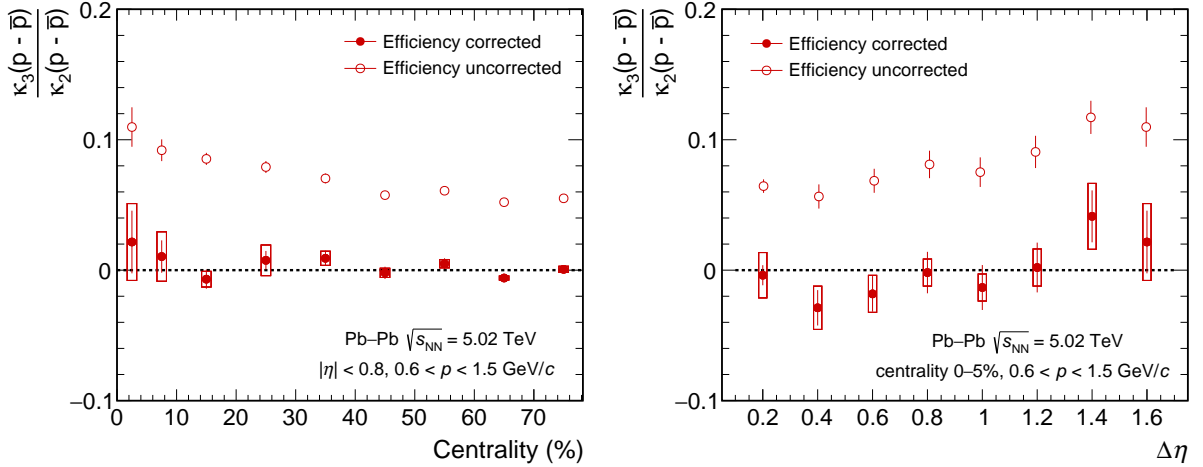


Figure 6: Centrality (left) and pseudorapidity interval (right) dependence of the ratio of third- to second-order cumulants for net protons at $\sqrt{s_{\text{NN}}} = 5.02 \text{ TeV}$ before (open markers) and after (closed markers) efficiency correction.

cumulant ratio with a value of zero, which is lower than the expectation from the EPOS and HIJING generators, is a confirmation that the proton-to-antiproton ratio is closer to unity than calculated by these generators and that the systematic uncertainties for these measurements are under good control. A value of κ_3/κ_2 consistent with zero within small uncertainties also indicates that μ_B is very close to zero at LHC energies.

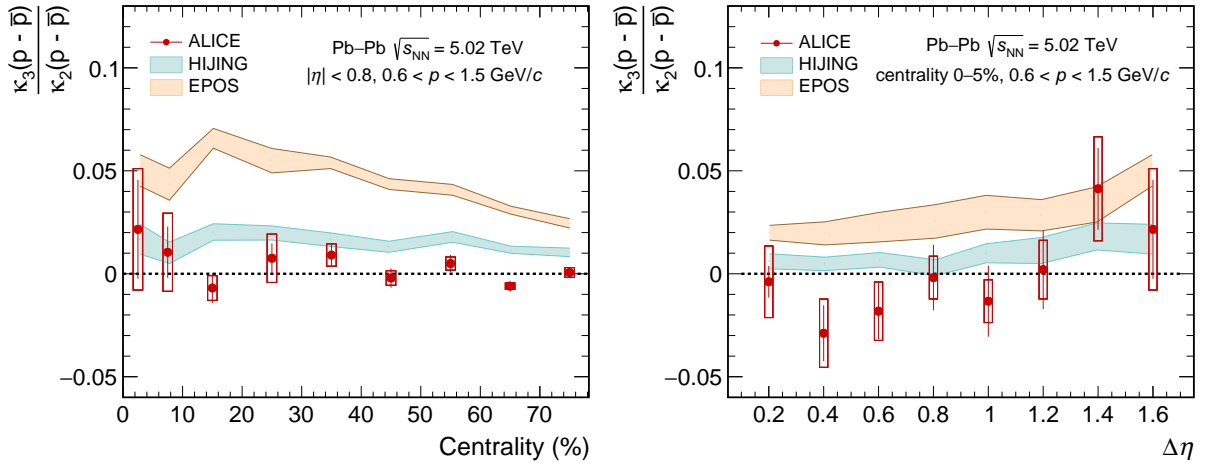


Figure 7: (Color online) Centrality (left) and pseudorapidity interval (right) dependence of the ratio of third- to second-order cumulants for net protons at $\sqrt{s_{\text{NN}}} = 5.02 \text{ TeV}$. The ALICE data are shown by red markers, while the colored shaded bands represent the results from HIJING [50] and EPOS [57] model calculations.

4 Conclusions

In summary, net-proton cumulant measurements up to third order and net-pion and net-kaon second-order cumulant measurements are reported. The technical challenges related to data analysis, in particular efficiency correction and event pile-up, are overcome as discussed in detail. Resonance contributions prove to be challenging in the study of fluctuations of the net-electric charge and the net-strangeness. A deviation of about 4% from the Skellam baseline is observed for the second-order net-proton cumulants for the widest $\Delta\eta$ interval. Investigation of this deviation in light of baryon number conservation led to the conclusion that the 2010 data from ALICE [30] indicate the presence of long-range rapidity corre-

lations between protons and antiprotons originating from the early phase of the collision. This finding is corroborated by the present analysis including the higher luminosity 2015 data with significantly different experimental conditions. Results of calculations using the HIJING generator, based on the Lund string model, reflect a much smaller correlation length of one unit of rapidity. This observed discrepancy calls into question the mechanism implemented in the Lund string model for the production of baryons. Baryon production as implemented in the EPOS event generator reflects the long-range correlation observed in the data. After accounting for the effect of baryon number conservation, the data from ALICE are consistent with LQCD expectations up to the third-order cumulants of the net protons. The finding of third-order net-proton cumulants consistent with zero with a precision of better than 4% is promising for the analysis of the higher-order cumulants during the operation of LHC with increased Pb–Pb luminosity [62] starting in 2022 and for the future heavy-ion detector planned for the early 2030s [63].

Acknowledgements

The ALICE Collaboration would like to thank all its engineers and technicians for their invaluable contributions to the construction of the experiment and the CERN accelerator teams for the outstanding performance of the LHC complex. The ALICE Collaboration gratefully acknowledges the resources and support provided by all Grid centres and the Worldwide LHC Computing Grid (WLCG) collaboration. The ALICE Collaboration acknowledges the following funding agencies for their support in building and running the ALICE detector: A. I. Alikhanyan National Science Laboratory (Yerevan Physics Institute) Foundation (ANSL), State Committee of Science and World Federation of Scientists (WFS), Armenia; Austrian Academy of Sciences, Austrian Science Fund (FWF): [M 2467-N36] and Nationalstiftung für Forschung, Technologie und Entwicklung, Austria; Ministry of Communications and High Technologies, National Nuclear Research Center, Azerbaijan; Conselho Nacional de Desenvolvimento Científico e Tecnológico (CNPq), Financiadora de Estudos e Projetos (Finep), Fundação de Amparo à Pesquisa do Estado de São Paulo (FAPESP) and Universidade Federal do Rio Grande do Sul (UFRGS), Brazil; Bulgarian Ministry of Education and Science, within the National Roadmap for Research Infrastructures 2020-2027 (object CERN), Bulgaria; Ministry of Education of China (MOEC) , Ministry of Science & Technology of China (MSTC) and National Natural Science Foundation of China (NSFC), China; Ministry of Science and Education and Croatian Science Foundation, Croatia; Centro de Aplicaciones Tecnológicas y Desarrollo Nuclear (CEADEN), Cubaenergía, Cuba; Ministry of Education, Youth and Sports of the Czech Republic, Czech Republic; The Danish Council for Independent Research | Natural Sciences, the VILLUM FONDEN and Danish National Research Foundation (DNRF), Denmark; Helsinki Institute of Physics (HIP), Finland; Commissariat à l’Energie Atomique (CEA) and Institut National de Physique Nucléaire et de Physique des Particules (IN2P3) and Centre National de la Recherche Scientifique (CNRS), France; Bundesministerium für Bildung und Forschung (BMBF) and GSI Helmholtzzentrum für Schwerionenforschung GmbH, Germany; General Secretariat for Research and Technology, Ministry of Education, Research and Religions, Greece; National Research, Development and Innovation Office, Hungary; Department of Atomic Energy Government of India (DAE), Department of Science and Technology, Government of India (DST), University Grants Commission, Government of India (UGC) and Council of Scientific and Industrial Research (CSIR), India; National Research and Innovation Agency - BRIN, Indonesia; Istituto Nazionale di Fisica Nucleare (INFN), Italy; Japanese Ministry of Education, Culture, Sports, Science and Technology (MEXT) and Japan Society for the Promotion of Science (JSPS) KAKENHI, Japan; Consejo Nacional de Ciencia (CONACYT) y Tecnología, through Fondo de Cooperación Internacional en Ciencia y Tecnología (FONCICYT) and Dirección General de Asuntos del Personal Académico (DGAPA), Mexico; Nederlandse Organisatie voor Wetenschappelijk Onderzoek (NWO), Netherlands; The Research Council of Norway, Norway; Commission on Science and Technology for Sustainable Development in the South (COMSATS), Pakistan; Pontificia Universidad Católica del Perú, Peru; Ministry of Education and Science, National Science Centre and WUT ID-UB, Poland; Korea Institute of Science and Technology Information and National

Research Foundation of Korea (NRF), Republic of Korea; Ministry of Education and Scientific Research, Institute of Atomic Physics, Ministry of Research and Innovation and Institute of Atomic Physics and University Politehnica of Bucharest, Romania; Ministry of Education, Science, Research and Sport of the Slovak Republic, Slovakia; National Research Foundation of South Africa, South Africa; Swedish Research Council (VR) and Knut & Alice Wallenberg Foundation (KAW), Sweden; European Organization for Nuclear Research, Switzerland; Suranaree University of Technology (SUT), National Science and Technology Development Agency (NSTDA), Thailand Science Research and Innovation (TSRI) and National Science, Research and Innovation Fund (NSRF), Thailand; Turkish Energy, Nuclear and Mineral Research Agency (TENMAK), Turkey; National Academy of Sciences of Ukraine, Ukraine; Science and Technology Facilities Council (STFC), United Kingdom; National Science Foundation of the United States of America (NSF) and United States Department of Energy, Office of Nuclear Physics (DOE NP), United States of America. In addition, individual groups or members have received support from: Marie Skłodowska Curie, European Research Council, Strong 2020 - Horizon 2020 (grant nos. 950692, 824093, 896850), European Union; Academy of Finland (Center of Excellence in Quark Matter) (grant nos. 346327, 346328), Finland; Programa de Apoyos para la Superación del Personal Académico, UNAM, Mexico.

References

- [1] E. V. Shuryak, “Quantum Chromodynamics and the Theory of Superdense Matter”, *Phys. Rept.* **61** (1980) 71.
- [2] H.-T. Ding, F. Karsch, and S. Mukherjee, “Thermodynamics of strong-interaction matter from Lattice QCD”, *Int. J. Mod. Phys. E* **24** (2015) 1530007, arXiv:1504.05274 [hep-lat].
- [3] S. Borsanyi, Z. Fodor, C. Hoelbling, S. D. Katz, S. Krieg, and K. K. Szabo, “Full result for the QCD equation of state with 2+1 flavors”, *Phys. Lett. B* **730** (2014) 99, arXiv:1309.5258 [hep-lat].
- [4] A. Andronic, P. Braun-Munzinger, K. Redlich, and J. Stachel, “Decoding the phase structure of QCD via particle production at high energy”, *Nature* **561** (2018) 321, arXiv:1710.09425 [nucl-th].
- [5] **HotQCD** Collaboration, A. Bazavov *et al.*, “Chiral crossover in QCD at zero and non-zero chemical potentials”, *Phys. Lett. B* **795** (2019) 15, arXiv:1812.08235 [hep-lat].
- [6] S. Borsanyi, Z. Fodor, J. N. Guenther, R. Kara, S. D. Katz, P. Parotto, A. Pasztor, C. Ratti, and K. K. Szabo, “QCD Crossover at Finite Chemical Potential from Lattice Simulations”, *Phys. Rev. Lett.* **125** (2020) 052001, arXiv:2002.02821 [hep-lat].
- [7] R. D. Pisarski and F. Wilczek, “Remarks on the Chiral Phase Transition in Chromodynamics”, *Phys. Rev. D* **29** (1984) 338.
- [8] X. Luo and N. Xu, “Search for the QCD Critical Point with Fluctuations of Conserved Quantities in Relativistic Heavy-Ion Collisions at RHIC : An Overview”, *Nucl. Sci. Tech.* **28** (2017) 112, arXiv:1701.02105 [nucl-ex].
- [9] N. Xu, “Exploration of the QCD Phase Diagram at Finite Baryon Density Region: Recent Results from RHIC Beam Energy Scan-I”, *Springer Proc. Phys.* **203** (2018) 1.
- [10] **NA49** Collaboration, T. Anticic *et al.*, “Search for the QCD critical point in nuclear collisions at the CERN SPS”, *Phys. Rev. C* **81** (2010) 064907, arXiv:0912.4198 [nucl-ex].

- [11] **CBM** Collaboration, T. Ablyazimov *et al.*, “Challenges in QCD matter physics –The scientific programme of the Compressed Baryonic Matter experiment at FAIR”, *Eur. Phys. J. A* **53** (2017) 60, arXiv:1607.01487 [nucl-ex].
- [12] **HotQCD** Collaboration, H. T. Ding *et al.*, “Chiral Phase Transition Temperature in (2+1)-Flavor QCD”, *Phys. Rev. Lett.* **123** (2019) 062002, arXiv:1903.04801 [hep-lat].
- [13] S. Borsanyi, Z. Fodor, J. N. Guenther, S. K. Katz, K. K. Szabo, A. Pasztor, I. Portillo, and C. Ratti, “Higher order fluctuations and correlations of conserved charges from lattice QCD”, *JHEP* **10** (2018) 205, arXiv:1805.04445 [hep-lat].
- [14] A. Bazavov *et al.*, “The chiral and deconfinement aspects of the QCD transition”, *Phys. Rev. D* **85** (2012) 054503, arXiv:1111.1710 [hep-lat].
- [15] **ALICE** Collaboration, E. Abbas *et al.*, “Centrality dependence of the pseudorapidity density distribution for charged particles in Pb-Pb collisions at $\sqrt{s_{\text{NN}}} = 2.76 \text{ TeV}$ ”, *Phys. Lett. B* **726** (2013) 610, arXiv:1304.0347 [nucl-ex].
- [16] B. Friman, F. Karsch, K. Redlich, and V. Skokov, “Fluctuations as probe of the QCD phase transition and freeze-out in heavy ion collisions at LHC and RHIC”, *Eur. Phys. J. C* **71** (2011) 1694, arXiv:1103.3511 [hep-ph].
- [17] F. Parisen Toldin, A. Pelissetto, and E. Vicari, “The 3-D O(4) universality class and the phase transition in two flavor QCD”, *JHEP* **07** (2003) 029, arXiv:hep-ph/0305264.
- [18] P. Braun-Munzinger, A. Rustamov, and J. Stachel, “Bridging the gap between event-by-event fluctuation measurements and theory predictions in relativistic nuclear collisions”, *Nucl. Phys. A* **960** (2017) 114, arXiv:1612.00702 [nucl-th].
- [19] R. V. Gavai and S. Gupta, “Lattice QCD predictions for shapes of event distributions along the freezeout curve in heavy-ion collisions”, *Phys. Lett. B* **696** (2011) 459, arXiv:1001.3796 [hep-lat].
- [20] S. Ejiri, F. Karsch, and K. Redlich, “Hadronic fluctuations at the QCD phase transition”, *Phys. Lett. B* **633** (2006) 275, arXiv:hep-ph/0509051.
- [21] A. Bzdak, V. Koch, and V. Skokov, “Baryon number conservation and the cumulants of the net proton distribution”, *Phys. Rev. C* **87** (2013) 014901, arXiv:1203.4529 [hep-ph].
- [22] P. Braun-Munzinger, A. Rustamov, and J. Stachel, “The role of the local conservation laws in fluctuations of conserved charges”, arXiv:1907.03032 [nucl-th].
- [23] V. Vovchenko and V. Koch, “Particilization of an interacting hadron resonance gas with global conservation laws for event-by-event fluctuations in heavy-ion collisions”, *Phys. Rev. C* **103** (2021) 044903, arXiv:2012.09954 [hep-ph].
- [24] Y. Ohnishi, M. Kitazawa, and M. Asakawa, “Thermal blurring of event-by-event fluctuations generated by rapidity conversion”, *Phys. Rev. C* **94** (2016) 044905, arXiv:1606.03827 [nucl-th].
- [25] M. Bluhm *et al.*, “Dynamics of critical fluctuations: Theory – phenomenology – heavy-ion collisions”, *Nucl. Phys. A* **1003** (2020) 122016, arXiv:2001.08831 [nucl-th].
- [26] C. Shen and B. Schenke, “Dynamical initial state model for relativistic heavy-ion collisions”, *Phys. Rev. C* **97** (2018) 024907, arXiv:1710.00881 [nucl-th].

- [27] O. Savchuk, V. Vovchenko, V. Koch, J. Steinheimer, and H. Stoecker, “Constraining baryon annihilation in the hadronic phase of heavy-ion collisions via event-by-event fluctuations”, *Phys. Lett. B* **827** (2022) 136983, arXiv:2106.08239 [hep-ph].
- [28] ALICE Collaboration, K. Aamodt *et al.*, “The ALICE experiment at the CERN LHC”, *JINST* **3** (2008) S08002.
- [29] ALICE Collaboration, B. B. Abelev *et al.*, “Performance of the ALICE Experiment at the CERN LHC”, *Int. J. Mod. Phys. A* **29** (2014) 1430044, arXiv:1402.4476 [nucl-ex].
- [30] ALICE Collaboration, S. Acharya *et al.*, “Global baryon number conservation encoded in net-proton fluctuations measured in Pb-Pb collisions at $\sqrt{s_{\text{NN}}} = 2.76 \text{ TeV}$ ”, *Phys. Lett. B* **807** (2020) 135564, arXiv:1910.14396 [nucl-ex].
- [31] ALICE Collaboration, S. Acharya *et al.*, “Relative particle yield fluctuations in Pb-Pb collisions at $\sqrt{s_{\text{NN}}} = 2.76 \text{ TeV}$ ”, *Eur. Phys. J. C* **79** (2019) 236, arXiv:1712.07929 [nucl-ex].
- [32] ALICE Collaboration, E. Abbas *et al.*, “Performance of the ALICE VZERO system”, *JINST* **8** (2013) P10016, arXiv:1306.3130 [nucl-ex].
- [33] ALICE Collaboration, B. Abelev *et al.*, “Centrality determination of Pb-Pb collisions at $\sqrt{s_{\text{NN}}} = 2.76 \text{ TeV}$ with ALICE”, *Phys. Rev. C* **88** (2013) 044909, arXiv:1301.4361 [nucl-ex].
- [34] C. Loizides, J. Nagle, and P. Steinberg, “Improved version of the PHOBOS Glauber Monte Carlo”, *SoftwareX* **1-2** (2015) 13, arXiv:1408.2549 [nucl-ex].
- [35] M. L. Miller, K. Reygers, S. J. Sanders, and P. Steinberg, “Glauber modeling in high energy nuclear collisions”, *Ann. Rev. Nucl. Part. Sci.* **57** (2007) 205, arXiv:nucl-ex/0701025.
- [36] J. Alme *et al.*, “The ALICE TPC, a large 3-dimensional tracking device with fast readout for ultra-high multiplicity events”, *Nucl. Instrum. Meth. A* **622** (2010) 316, arXiv:1001.1950 [physics.ins-det].
- [37] ALICE Collaboration, “ALICE Inner Tracking System (ITS): Technical Design Report”, *CERN-LHCC-99-012* (1999). <http://cds.cern.ch/record/391175>.
- [38] ALICE Collaboration, K. Aamodt *et al.*, “Alignment of the ALICE Inner Tracking System with cosmic-ray tracks”, *JINST* **5** (2010) P03003, arXiv:1001.0502 [physics.ins-det].
- [39] ALICE Collaboration, G. Dellacasa *et al.*, “ALICE technical design report of the zero degree calorimeter (ZDC)”, *CERN-LHCC-99-005* (1999). <https://cds.cern.ch/record/381433>.
- [40] M. Arslanbek, E. Hellbär, M. Ivanov, R. H. Münzer, and J. Wiechula, “Track Reconstruction in a High-Density Environment with ALICE”, *Particles* **5** (2022) 84, arXiv:2203.10325 [physics.ins-det].
- [41] ALICE Collaboration, K. Aamodt *et al.*, “Suppression of Charged Particle Production at Large Transverse Momentum in Central Pb-Pb Collisions at $\sqrt{s_{\text{NN}}} = 2.76 \text{ TeV}$ ”, *Phys. Lett. B* **696** (2011) 30, arXiv:1012.1004 [nucl-ex].
- [42] M. Gazdzicki, K. Grebieszkow, M. Mackowiak, and S. Mrowczynski, “Identity method to study chemical fluctuations in relativistic heavy-ion collisions”, *Phys. Rev. C* **83** (2011) 054907, arXiv:1103.2887 [nucl-th].
- [43] A. Rustamov and M. I. Gorenstein, “Identity method for the determination of the moments of multiplicity distributions”, *Phys. Rev. C* **86** (2012) 044906, arXiv:1204.6632 [nucl-th].

- [44] M. Arslanbekov and A. Rustamov, “TIdentity module for the reconstruction of the moments of multiplicity distributions”, *Nucl. Instrum. Meth. A* **946** (2019) 162622, arXiv:1807.06370 [hep-ex].
- [45] A. Bzdak and V. Koch, “Acceptance corrections to net baryon and net charge cumulants”, *Phys. Rev. C* **86** (2012) 044904, arXiv:1206.4286 [nucl-th].
- [46] A. Bzdak and V. Koch, “Local Efficiency Corrections to Higher Order Cumulants”, *Phys. Rev. C* **91** (2015) 027901, arXiv:1312.4574 [nucl-th].
- [47] T. Nonaka, M. Kitazawa, and S. Esumi, “More efficient formulas for efficiency correction of cumulants and effect of using averaged efficiency”, *Phys. Rev. C* **95** (2017) 064912, arXiv:1702.07106 [physics.data-an]. [Erratum: Phys.Rev.C 103, 029901 (2021)].
- [48] A. Pandav, D. Mallick, and B. Mohanty, “Effect of limited statistics on higher order cumulants measurement in heavy-ion collision experiments”, *Nucl. Phys. A* **991** (2019) 121608, arXiv:1809.08892 [nucl-ex].
- [49] **GEANT4** Collaboration, S. Agostinelli *et al.*, “GEANT4—a simulation toolkit”, *Nucl. Instrum. Meth. A* **506** (2003) 250–303.
- [50] M. Gyulassy and X.-N. Wang, “HIJING 1.0: A Monte Carlo program for parton and particle production in high-energy hadronic and nuclear collisions”, *Comput. Phys. Commun.* **83** (1994) 307, arXiv:nucl-th/9502021.
- [51] M. Kitazawa and M. Asakawa, “Relation between baryon number fluctuations and experimentally observed proton number fluctuations in relativistic heavy ion collisions”, *Phys. Rev. C* **86** (2012) 024904, arXiv:1205.3292 [nucl-th]. [Erratum: Phys.Rev.C 86, 069902 (2012)].
- [52] P. Braun-Munzinger, B. Friman, F. Karsch, K. Redlich, and V. Skokov, “Net-charge probability distributions in heavy ion collisions at chemical freeze-out”, *Nucl. Phys. A* **880** (2012) 48, arXiv:1111.5063 [hep-ph].
- [53] J. G. Skellam, “The frequency distribution of the difference between two Poisson variates belonging to different populations”, *J. Royal Stat. Soc. A* **109(3)** (1946) 296.
- [54] **ALICE** Collaboration, B. Abelev *et al.*, “Centrality dependence of π , K, p production in Pb-Pb collisions at $\sqrt{s_{\text{NN}}} = 2.76$ TeV”, *Phys. Rev. C* **88** (2013) 044910, arXiv:1303.0737 [hep-ex].
- [55] A. Bazavov *et al.*, “Skewness, kurtosis, and the fifth and sixth order cumulants of net baryon-number distributions from lattice QCD confront high-statistics STAR data”, *Phys. Rev. D* **101** (2020) 074502, arXiv:2001.08530 [hep-lat].
- [56] P. Braun-Munzinger, B. Friman, K. Redlich, A. Rustamov, and J. Stachel, “Relativistic nuclear collisions: Establishing a non-critical baseline for fluctuation measurements”, *Nucl. Phys. A* **1008** (2021) 122141, arXiv:2007.02463 [nucl-th].
- [57] T. Pierog, I. Karpenko, J. M. Katzy, E. Yatsenko, and K. Werner, “EPOS LHC: Test of collective hadronization with data measured at the CERN Large Hadron Collider”, *Phys. Rev. C* **92** (2015) 034906, arXiv:1306.0121 [hep-ph].
- [58] A. Dumitru, F. Gelis, L. McLerran, and R. Venugopalan, “Glasma flux tubes and the near side ridge phenomenon at RHIC”, *Nucl. Phys. A* **810** (2008) 91, arXiv:0804.3858 [hep-ph].
- [59] B. Andersson, G. Gustafson, G. Ingelman, and T. Sjostrand, “Parton Fragmentation and String Dynamics”, *Phys. Rept.* **97** (1983) 31–145.

- [60] P. Braun-Munzinger, A. Rustamov, and J. Stachel, “Experimental results on fluctuations of conserved charges confronted with predictions from canonical thermodynamics”, *Nucl. Phys. A* **982** (2019) 307, arXiv:1807.08927 [nucl-th].
- [61] **HotQCD** Collaboration, A. Bazavov *et al.*, “Skewness and kurtosis of net baryon-number distributions at small values of the baryon chemical potential”, *Phys. Rev. D* **96** (2017) 074510, arXiv:1708.04897 [hep-lat].
- [62] Z. Citron *et al.*, “Report from Working Group 5: Future physics opportunities for high-density QCD at the LHC with heavy-ion and proton beams”, *CERN Yellow Rep. Monogr.* **7** (2019) 1159, arXiv:1812.06772 [hep-ph].
- [63] **ALICE** Collaboration, “Letter of intent for ALICE 3: A next generation heavy-ion experiment at the LHC”, *CERN-LHCC-2022-009, LHCC-I-038* (2022) .
<http://cds.cern.ch/record/2803563>.

A The ALICE Collaboration

- S. Acharya ^{125,132}, D. Adamová ⁸⁶, A. Adler⁶⁹, G. Aglieri Rinella ³², M. Agnello ²⁹, N. Agrawal ⁵⁰, Z. Ahammed ¹³², S. Ahmad ¹⁵, S.U. Ahn ⁷⁰, I. Ahuja ³⁷, A. Akindinov ¹⁴⁰, M. Al-Turany ⁹⁸, D. Aleksandrov ¹⁴⁰, B. Alessandro ⁵⁵, H.M. Alfanda ⁶, R. Alfaro Molina ⁶⁶, B. Ali ¹⁵, Y. Ali ¹³, A. Alici ²⁵, N. Alizadehvandchali ¹¹⁴, A. Alkin ³², J. Alme ²⁰, G. Alocço ⁵¹, T. Alt ⁶³, I. Altsybeev ¹⁴⁰, M.N. Anaam ⁶, C. Andrei ⁴⁵, A. Andronic ¹³⁵, V. Anguelov ⁹⁵, F. Antinori ⁵³, P. Antonioli ⁵⁰, C. Anuj ¹⁵, N. Apadula ⁷⁴, L. Aphecetche ¹⁰⁴, H. Appelshäuser ⁶³, C. Arata ⁷³, S. Arcelli ²⁵, R. Arnaldi ⁵⁵, I.C. Arsene ¹⁹, M. Arslanbekov ¹³⁷, A. Augustinus ³², R. Averbeck ⁹⁸, S. Aziz ⁷², M.D. Azmi ¹⁵, A. Badalà ⁵², Y.W. Baek ⁴⁰, X. Bai ¹¹⁸, R. Bailhache ⁶³, Y. Bailung ⁴⁷, R. Bala ⁹¹, A. Balbino ²⁹, A. Baldissari ¹²⁸, B. Balis ², D. Banerjee ⁴, Z. Banoo ⁹¹, R. Barbera ²⁶, L. Barioglio ⁹⁶, M. Barlou ⁷⁸, G.G. Barnaföldi ¹³⁶, L.S. Barnby ⁸⁵, V. Barret ¹²⁵, L. Barreto ¹¹⁰, C. Bartels ¹¹⁷, K. Barth ³², E. Bartsch ⁶³, F. Baruffaldi ²⁷, N. Bastid ¹²⁵, S. Basu ⁷⁵, G. Batigne ¹⁰⁴, D. Battistini ⁹⁶, B. Batyunya ¹⁴¹, D. Bauri ⁴⁶, J.L. Bazo Alba ¹⁰², I.G. Bearden ⁸³, C. Beattie ¹³⁷, P. Becht ⁹⁸, D. Behera ⁴⁷, I. Belikov ¹²⁷, A.D.C. Bell Hechavarria ¹³⁵, F. Bellini ²⁵, R. Bellwied ¹¹⁴, S. Belokurova ¹⁴⁰, V. Belyaev ¹⁴⁰, G. Bencedi ^{136,64}, S. Beole ²⁴, A. Bercuci ⁴⁵, Y. Berdnikov ¹⁴⁰, A. Berdnikova ⁹⁵, L. Bergmann ⁹⁵, M.G. Besouï ⁶², L. Betev ³², P.P. Bhaduri ¹³², A. Bhasin ⁹¹, M.A. Bhat ⁴, B. Bhattacharjee ⁴¹, L. Bianchi ²⁴, N. Bianchi ⁴⁸, J. Bielčík ³⁵, J. Bielčíková ⁸⁶, J. Biernat ¹⁰⁷, A.P. Bigot ¹²⁷, A. Bilandzic ⁹⁶, G. Biro ¹³⁶, S. Biswas ⁴, N. Bize ¹⁰⁴, J.T. Blair ¹⁰⁸, D. Blau ¹⁴⁰, M.B. Blidaru ⁹⁸, N. Bluhme ³⁸, C. Blume ⁶³, G. Boca ^{21,54}, F. Bock ⁸⁷, T. Bodova ²⁰, A. Bogdanov ¹⁴⁰, S. Boi ²², J. Bok ⁵⁷, L. Boldizsár ¹³⁶, A. Bolozdynya ¹⁴⁰, M. Bombara ³⁷, P.M. Bond ³², G. Bonomi ^{131,54}, H. Borel ¹²⁸, A. Borissov ¹⁴⁰, H. Bossi ¹³⁷, E. Botta ²⁴, L. Bratrud ⁶³, P. Braun-Munzinger ⁹⁸, M. Bregant ¹¹⁰, M. Broz ³⁵, G.E. Bruno ^{97,31}, M.D. Buckland ¹¹⁷, D. Budnikov ¹⁴⁰, H. Buesching ⁶³, S. Bufalino ²⁹, O. Bugnon ¹⁰⁴, P. Buhler ¹⁰³, Z. Buthelezi ^{67,121}, J.B. Butt ¹³, A. Bylinkin ¹¹⁶, S.A. Bysiak ¹⁰⁷, M. Cai ^{27,6}, H. Caines ¹³⁷, A. Caliva ⁹⁸, E. Calvo Villar ¹⁰², J.M.M. Camacho ¹⁰⁹, P. Camerini ²³, F.D.M. Canedo ¹¹⁰, M. Carabas ¹²⁴, F. Carnesecchi ³², R. Caron ¹²⁶, J. Castillo Castellanos ¹²⁸, F. Catalano ²⁹, C. Ceballos Sanchez ¹⁴¹, I. Chakaberia ⁷⁴, P. Chakraborty ⁴⁶, S. Chandra ¹³², S. Chapelard ³², M. Chartier ¹¹⁷, S. Chattopadhyay ¹³², S. Chattopadhyay ¹⁰⁰, T.G. Chavez ⁴⁴, T. Cheng ⁶, C. Cheshkov ¹²⁶, B. Cheynis ¹²⁶, V. Chibante Barroso ³², D.D. Chinellato ¹¹¹, E.S. Chizzali ^{II,96}, J. Cho ⁵⁷, S. Cho ⁵⁷, P. Chochula ³², P. Christakoglou ⁸⁴, C.H. Christensen ⁸³, P. Christiansen ⁷⁵, T. Chujo ¹²³, M. Ciacco ²⁹, C. Cicalo ⁵¹, L. Cifarelli ²⁵, F. Cindolo ⁵⁰, M.R. Ciupé ⁹⁸, G. Clai^{III,50}, F. Colamaria ⁴⁹, J.S. Colburn ¹⁰¹, D. Colella ^{97,31}, A. Collu ⁷⁴, M. Colocci ³², M. Concas ^{IV,55}, G. Conesa Balbastre ⁷³, Z. Conesa del Valle ⁷², G. Contin ²³, J.G. Contreras ³⁵, M.L. Coquet ¹²⁸, T.M. Cormier ^{I,87}, P. Cortese ^{130,55}, M.R. Cosentino ¹¹², F. Costa ³², S. Costanza ^{21,54}, P. Crochet ¹²⁵, R. Cruz-Torres ⁷⁴, E. Cuautle ⁶⁴, P. Cui ⁶, L. Cunqueiro ⁸⁷, A. Dainese ⁵³, M.C. Danisch ⁹⁵, A. Danu ⁶², P. Das ⁸⁰, P. Das ⁴, S. Das ⁴, A.R. Dash ¹³⁵, S. Dash ⁴⁶, R.M.H. David ⁴⁴, A. De Caro ²⁸, G. de Cataldo ⁴⁹, L. De Cilladi ²⁴, J. de Cuveland ³⁸, A. De Falco ²², D. De Gruttola ²⁸, N. De Marco ⁵⁵, C. De Martin ²³, S. De Pasquale ²⁸, S. Deb ⁴⁷, H.F. Degenhardt ¹¹⁰, K.R. Deja ¹³³, R. Del Grande ⁹⁶, L. Dello Stritto ²⁸, W. Deng ⁶, P. Dhankher ¹⁸, D. Di Bari ³¹, A. Di Mauro ³², R.A. Diaz ^{141,7}, T. Dietel ¹¹³, Y. Ding ^{126,6}, R. Divià ³², D.U. Dixit ¹⁸, Ø. Djupsland ²⁰, U. Dmitrieva ¹⁴⁰, A. Dobrin ⁶², B. Dönigus ⁶³, A.K. Dubey ¹³², J.M. Dubinski ¹³³, A. Dubla ⁹⁸, S. Dudi ⁹⁰, P. Dupieux ¹²⁵, M. Durkac ¹⁰⁶, N. Dzalaiova ¹², T.M. Eder ¹³⁵, R.J. Ehlers ⁸⁷, V.N. Eikeland ²⁰, F. Eisenhut ⁶³, D. Elia ⁴⁹, B. Erazmus ¹⁰⁴, F. Ercolelli ²⁵, F. Erhardt ⁸⁹, M.R. Ersdal ²⁰, B. Espagnon ⁷², G. Eulisse ³², D. Evans ¹⁰¹, S. Evdokimov ¹⁴⁰, L. Fabbietti ⁹⁶, M. Faggin ²⁷, J. Faivre ⁷³, F. Fan ⁶, W. Fan ⁷⁴, A. Fantoni ⁴⁸, M. Fasel ⁸⁷, P. Fecchio ²⁹, A. Feliciello ⁵⁵, G. Feofilov ¹⁴⁰, A. Fernández Téllez ⁴⁴, M.B. Ferrer ³², A. Ferrero ¹²⁸, A. Ferretti ²⁴, V.J.G. Feuillard ⁹⁵, J. Figiel ¹⁰⁷, V. Filova ³⁵, D. Finogeev ¹⁴⁰, F.M. Fionda ⁵¹, G. Fiorenza ⁹⁷, F. Flor ¹¹⁴, A.N. Flores ¹⁰⁸, S. Foertsch ⁶⁷, I. Fokin ⁹⁵, S. Fokin ¹⁴⁰, E. Fragiaco ⁵⁶, E. Frajna ¹³⁶, U. Fuchs ³², N. Funicello ²⁸, C. Furget ⁷³, A. Furs ¹⁴⁰, T. Fusayasu ⁹⁹, J.J. Gaardhøje ⁸³, M. Gagliardi ²⁴, A.M. Gago ¹⁰², A. Gal ¹²⁷, C.D. Galvan ¹⁰⁹, D.R. Gangadharan ¹¹⁴, P. Ganoti ⁷⁸, C. Garabatos ⁹⁸, J.R.A. Garcia ⁴⁴, E. Garcia-Solis ⁹, K. Garg ¹⁰⁴, C. Gargiulo ³², A. Garibaldi ⁸¹, K. Garner ¹³⁵, A. Gautam ¹¹⁶, M.B. Gay Ducati ⁶⁵, M. Germain ¹⁰⁴, C. Ghosh ¹³², S.K. Ghosh ⁴, M. Giacalone ²⁵, P. Gianotti ⁴⁸, P. Giubellino ^{98,55}, P. Giubilato ²⁷, A.M.C. Glaenzer ¹²⁸, P. Glässel ⁹⁵, E. Glimos ¹²⁰, D.J.Q. Goh ⁷⁶, V. Gonzalez ¹³⁴, L.H. González-Trueba ⁶⁶, M. Gorgon ², L. Görlich ¹⁰⁷, S. Gotovac ³³, V. Grabski ⁶⁶, L.K. Graczykowski ¹³³, E. Grecka ⁸⁶, L. Greiner ⁷⁴, A. Grelli ⁵⁸, C. Grigoras ³², V. Grigoriev ¹⁴⁰, S. Grigoryan ^{141,1}, F. Grossa ³², J.F. Grosse-Oetringhaus ³², R. Grossi ⁹⁸, D. Grund ³⁵,

- G.G. Guardiano ¹¹¹, R. Guernane ⁷³, M. Guilbaud ¹⁰⁴, K. Gulbrandsen ⁸³, T. Gunji ¹²², W. Guo ⁶,
 A. Gupta ⁹¹, R. Gupta ⁹¹, S.P. Guzman ⁴⁴, L. Gyulai ¹³⁶, M.K. Habib ⁹⁸, C. Hadjidakis ⁷²,
 H. Hamagaki ⁷⁶, M. Hamid ⁶, Y. Han ¹³⁸, R. Hannigan ¹⁰⁸, M.R. Haque ¹³³, A. Harlenderova ⁹⁸,
 J.W. Harris ¹³⁷, A. Harton ⁹, H. Hassan ⁸⁷, D. Hatzifotiadou ⁵⁰, P. Hauer ⁴², L.B. Havener ¹³⁷,
 S.T. Heckel ⁹⁶, E. Hellbär ⁹⁸, H. Helstrup ³⁴, T. Herman ³⁵, G. Herrera Corral ⁸, F. Herrmann ¹³⁵,
 S. Herrmann ¹²⁶, K.F. Hetland ³⁴, B. Heybeck ⁶³, H. Hillemanns ³², C. Hills ¹¹⁷, B. Hippolyte ¹²⁷,
 B. Hofman ⁵⁸, B. Hohlweger ⁸⁴, J. Honermann ¹³⁵, G.H. Hong ¹³⁸, D. Horak ³⁵, A. Horzyk ²,
 R. Hosokawa ¹⁴, Y. Hou ⁶, P. Hristov ³², C. Hughes ¹²⁰, P. Huhn ⁶³, L.M. Huhta ¹¹⁵, C.V. Hulse ⁷²,
 T.J. Humanic ⁸⁸, H. Hushnud ¹⁰⁰, A. Hutson ¹¹⁴, D. Hutter ³⁸, J.P. Iddon ¹¹⁷, R. Ilkaev ¹⁴⁰, H. Ilyas ¹³,
 M. Inaba ¹²³, G.M. Innocenti ³², M. Ippolitov ¹⁴⁰, A. Isakov ⁸⁶, T. Isidori ¹¹⁶, M.S. Islam ¹⁰⁰,
 M. Ivanov ¹², M. Ivanov ⁹⁸, V. Ivanov ¹⁴⁰, V. Izucheev ¹⁴⁰, M. Jablonski ², B. Jacak ⁷⁴, N. Jacazio ³²,
 P.M. Jacobs ⁷⁴, S. Jadlovska ¹⁰⁶, J. Jadlovsky ¹⁰⁶, S. Jaelani ⁸², L. Jaffe ³⁸, C. Jahnke ¹¹¹, M.A. Janik ¹³³,
 T. Janson ⁶⁹, M. Jercic ⁸⁹, O. Jevons ¹⁰¹, A.A.P. Jimenez ⁶⁴, F. Jonas ⁸⁷, P.G. Jones ¹⁰¹, J.M. Jowett ^{32,98},
 J. Jung ⁶³, M. Jung ⁶³, A. Junique ³², A. Jusko ¹⁰¹, M.J. Kabus ^{32,133}, J. Kaewjai ¹⁰⁵, P. Kalinak ⁵⁹,
 A.S. Kalteyer ⁹⁸, A. Kalweit ³², V. Kaplin ¹⁴⁰, A. Karasu Uysal ⁷¹, D. Karatovic ⁸⁹, O. Karavichev ¹⁴⁰,
 T. Karavicheva ¹⁴⁰, P. Karczmarczyk ¹³³, E. Karpechev ¹⁴⁰, V. Kashyap ⁸⁰, A. Kazantsev ¹⁴⁰,
 U. Kebschull ⁶⁹, R. Keidel ¹³⁹, D.L.D. Keijdener ⁵⁸, M. Keil ³², B. Ketzer ⁴², A.M. Khan ⁶, S. Khan ¹⁵,
 A. Khanzadeev ¹⁴⁰, Y. Kharlov ¹⁴⁰, A. Khatun ¹⁵, A. Khuntia ¹⁰⁷, B. Kileng ³⁴, B. Kim ¹⁶,
 C. Kim ¹⁶, D.J. Kim ¹¹⁵, E.J. Kim ⁶⁸, J. Kim ¹³⁸, J.S. Kim ⁴⁰, J. Kim ⁹⁵, J. Kim ⁶⁸, M. Kim ⁹⁵,
 S. Kim ¹⁷, T. Kim ¹³⁸, K. Kimura ⁹³, S. Kirsch ⁶³, I. Kisel ³⁸, S. Kiselev ¹⁴⁰, A. Kisiel ¹³³,
 J.P. Kitowski ², J.L. Klay ⁵, J. Klein ³², S. Klein ⁷⁴, C. Klein-Bösing ¹³⁵, M. Kleiner ⁶³,
 T. Klemenz ⁹⁶, A. Kluge ³², A.G. Knospe ¹¹⁴, C. Kobdaj ¹⁰⁵, T. Kollegger ⁹⁸, A. Kondratyev ¹⁴¹,
 E. Kondratyuk ¹⁴⁰, J. Konig ⁶³, S.A. Konigstorfer ⁹⁶, P.J. Konopka ³², G. Kornakov ¹³³,
 S.D. Koryciak ², A. Kotliarov ⁸⁶, O. Kovalenko ⁷⁹, V. Kovalenko ¹⁴⁰, M. Kowalski ¹⁰⁷, I. Králik ⁵⁹,
 A. Kravčáková ³⁷, L. Kreis ⁹⁸, M. Krivda ^{101,59}, F. Krizek ⁸⁶, K. Krizkova Gajdosova ³⁵, M. Kroesen ⁹⁵,
 M. Krüger ⁶³, D.M. Krupova ³⁵, E. Kryshen ¹⁴⁰, M. Krzewicki ³⁸, V. Kučera ³², C. Kuhn ¹²⁷,
 P.G. Kuijer ⁸⁴, T. Kumaoka ¹²³, D. Kumar ¹³², L. Kumar ⁹⁰, N. Kumar ⁹⁰, S. Kumar ³¹, S. Kundu ³²,
 P. Kurashvili ⁷⁹, A. Kurepin ¹⁴⁰, A.B. Kurepin ¹⁴⁰, S. Kushpil ⁸⁶, J. Kvapil ¹⁰¹, M.J. Kweon ⁵⁷,
 J.Y. Kwon ⁵⁷, Y. Kwon ¹³⁸, S.L. La Pointe ³⁸, P. La Rocca ²⁶, Y.S. Lai ⁷⁴, A. Lakrathok ¹⁰⁵,
 M. Lamanna ³², R. Langoy ¹¹⁹, P. Larionov ⁴⁸, E. Laudi ³², L. Lautner ^{32,96}, R. Lavicka ¹⁰³,
 T. Lazareva ¹⁴⁰, R. Lea ^{131,54}, G. Legras ¹³⁵, J. Lehrbach ³⁸, R.C. Lemmon ⁸⁵, I. León Monzón ¹⁰⁹,
 M.M. Lesch ⁹⁶, E.D. Lesser ¹⁸, M. Lettrich ⁹⁶, P. Lévai ¹³⁶, X. Li ¹⁰, X.L. Li ⁶, J. Lien ¹¹⁹, R. Lietava ¹⁰¹,
 B. Lim ¹⁶, S.H. Lim ¹⁶, V. Lindenstruth ³⁸, A. Lindner ⁴⁵, C. Lippmann ⁹⁸, A. Liu ¹⁸, D.H. Liu ⁶,
 J. Liu ¹¹⁷, I.M. Lofnes ²⁰, C. Loizides ⁸⁷, P. Loncar ³³, J.A. Lopez ⁹⁵, X. Lopez ¹²⁵, E. López
 Torres ⁷, P. Lu ^{98,118}, J.R. Luhder ¹³⁵, M. Lunardon ²⁷, G. Luparello ⁵⁶, Y.G. Ma ³⁹, A. Maevskaya ¹⁴⁰,
 M. Mager ³², T. Mahmoud ⁴², A. Maire ¹²⁷, M. Malaeve ¹⁴⁰, G. Malfattore ²⁵, N.M. Malik ⁹¹,
 Q.W. Malik ¹⁹, S.K. Malik ⁹¹, L. Malinina ^{VII,141}, D. Mal'Kevich ¹⁴⁰, D. Mallick ⁸⁰, N. Mallick ⁴⁷,
 G. Mandaglio ^{30,52}, V. Manko ¹⁴⁰, F. Manso ¹²⁵, V. Manzari ⁴⁹, Y. Mao ⁶, G.V. Margagliotti ²³,
 A. Margotti ⁵⁰, A. Marín ⁹⁸, C. Markert ¹⁰⁸, M. Marquard ⁶³, P. Martinengo ³², J.L. Martinez ¹¹⁴,
 M.I. Martínez ⁴⁴, G. Martínez García ¹⁰⁴, S. Masciocchi ⁹⁸, M. Masera ²⁴, A. Masoni ⁵¹,
 L. Massacrier ⁷², A. Mastroserio ^{129,49}, A.M. Mathis ⁹⁶, O. Matonoha ⁷⁵, P.F.T. Matuoka ¹¹⁰,
 A. Matyja ¹⁰⁷, C. Mayer ¹⁰⁷, A.L. Mazuecos ³², F. Mazzaschi ²⁴, M. Mazzilli ³², J.E. Mdhluli ¹²¹,
 A.F. Mechler ⁶³, Y. Melikyan ¹⁴⁰, A. Menchaca-Rocha ⁶⁶, E. Meninno ^{103,28}, A.S. Menon ¹¹⁴,
 M. Meres ¹², S. Mhlanga ^{113,67}, Y. Miake ¹²³, L. Micheletti ⁵⁵, L.C. Migliorin ¹²⁶, D.L. Mihaylov ⁹⁶,
 K. Mikhaylov ^{141,140}, A.N. Mishra ¹³⁶, D. Miśkowiec ⁹⁸, A. Modak ⁴, A.P. Mohanty ⁵⁸, B. Mohanty ⁸⁰,
 M. Mohisin Khan ^{V,15}, M.A. Molander ⁴³, Z. Moravcova ⁸³, C. Mordasini ⁹⁶, D.A. Moreira De
 Godoy ¹³⁵, I. Morozov ¹⁴⁰, A. Morsch ³², T. Mrnjavac ³², V. Muccifora ⁴⁸, S. Muhuri ¹³²,
 J.D. Mulligan ⁷⁴, A. Mulliri ²², M.G. Munhoz ¹¹⁰, R.H. Munzer ⁶³, H. Murakami ¹²², S. Murray ¹¹³,
 L. Musa ³², J. Musinsky ⁵⁹, J.W. Myrcha ¹³³, B. Naik ¹²¹, R. Nair ⁷⁹, A.I. Nambrath ¹⁸,
 B.K. Nandi ⁴⁶, R. Nania ⁵⁰, E. Nappi ⁴⁹, A.F. Nassirpour ⁷⁵, A. Nath ⁹⁵, C. Nattrass ¹²⁰,
 T.K. Nayak ⁸⁰, A. Neagu ¹⁹, A. Negru ¹²⁴, L. Nellen ⁶⁴, S.V. Nesbo ³⁴, G. Neskovic ³⁸, D. Nesterov ¹⁴⁰,
 B.S. Nielsen ⁸³, E.G. Nielsen ⁸³, S. Nikolaev ¹⁴⁰, S. Nikulin ¹⁴⁰, V. Nikulin ¹⁴⁰, F. Noferini ⁵⁰,
 S. Noh ¹¹, P. Nomokonov ¹⁴¹, J. Norman ¹¹⁷, N. Novitzky ¹²³, P. Nowakowski ¹³³, A. Nyanin ¹⁴⁰,
 J. Nystrand ²⁰, M. Ogino ⁷⁶, A. Ohlson ⁷⁵, V.A. Okorokov ¹⁴⁰, J. Oleniacz ¹³³, A.C. Oliveira Da
 Silva ¹²⁰, M.H. Oliver ¹³⁷, A. Onnerstad ¹¹⁵, C. Oppedisano ⁵⁵, A. Ortiz Velasquez ⁶⁴, A. Oskarsson ⁷⁵,
 J. Otwinowski ¹⁰⁷, M. Oya ⁹³, K. Oyama ⁷⁶, Y. Pachmayer ⁹⁵, S. Padhan ⁴⁶, D. Pagano ^{131,54},

- G. Paić ⁶⁴, A. Palasciano ⁴⁹, S. Panebianco ¹²⁸, H. Park ¹²³, J. Park ⁵⁷, J.E. Parkkila ^{32,115}, S.P. Pathak ¹¹⁴, R.N. Patra ⁹¹, B. Paul ²², H. Pei ⁶, T. Peitzmann ⁵⁸, X. Peng ⁶, M. Pennisi ²⁴, L.G. Pereira ⁶⁵, H. Pereira Da Costa ¹²⁸, D. Peresunko ¹⁴⁰, G.M. Perez ⁷, S. Perrin ¹²⁸, Y. Pestov ¹⁴⁰, V. Petráček ³⁵, V. Petrov ¹⁴⁰, M. Petrovici ⁴⁵, R.P. Pezzi ^{104,65}, S. Piano ⁵⁶, M. Pikna ¹², P. Pillot ¹⁰⁴, O. Pinazza ^{50,32}, L. Pinsky ¹¹⁴, C. Pinto ⁹⁶, S. Pisano ⁴⁸, M. Płoskoń ⁷⁴, M. Planinic ⁸⁹, F. Pliquet ⁶³, M.G. Poghosyan ⁸⁷, S. Politano ²⁹, N. Poljak ⁸⁹, A. Pop ⁴⁵, S. Porteboeuf-Houssais ¹²⁵, J. Porter ⁷⁴, V. Pozdniakov ¹⁴¹, S.K. Prasad ⁴, S. Prasad ⁴⁷, R. Preghenella ⁵⁰, F. Prino ⁵⁵, C.A. Pruneau ¹³⁴, I. Pshenichnov ¹⁴⁰, M. Puccio ³², S. Pucillo ²⁴, Z. Pugelova ¹⁰⁶, S. Qiu ⁸⁴, L. Quaglia ²⁴, R.E. Quishpe ¹¹⁴, S. Ragoni ¹⁰¹, A. Rakotozafindrabe ¹²⁸, L. Ramello ^{130,55}, F. Rami ¹²⁷, S.A.R. Ramirez ⁴⁴, T.A. Rancien ⁷³, R. Raniwala ⁹², S. Raniwala ⁹², S.S. Räsänen ⁴³, R. Rath ^{50,47}, I. Ravasenga ⁸⁴, K.F. Read ^{87,120}, A.R. Redelbach ³⁸, K. Redlich ^{VI,79}, A. Rehman ²⁰, P. Reichelt ⁶³, F. Reidt ³², H.A. Reme-Ness ³⁴, Z. Rescakova ³⁷, K. Reygers ⁹⁵, A. Riabov ¹⁴⁰, V. Riabov ¹⁴⁰, R. Ricci ²⁸, T. Richert ⁷⁵, M. Richter ¹⁹, A.A. Riedel ⁹⁶, W. Riegler ³², F. Riggi ²⁶, C. Ristea ⁶², M. Rodríguez Cahuantzi ⁴⁴, K. Røed ¹⁹, R. Rogalev ¹⁴⁰, E. Rogochaya ¹⁴¹, T.S. Rogoschinski ⁶³, D. Rohr ³², D. Röhrich ²⁰, P.F. Rojas ⁴⁴, S. Rojas Torres ³⁵, P.S. Rokita ¹³³, G. Romanenko ¹⁴¹, F. Ronchetti ⁴⁸, A. Rosano ^{30,52}, E.D. Rosas ⁶⁴, A. Rossi ⁵³, A. Roy ⁴⁷, P. Roy ¹⁰⁰, S. Roy ⁴⁶, N. Rubini ²⁵, O.V. Rueda ⁷⁵, D. Ruggiano ¹³³, R. Rui ²³, B. Rumyantsev ¹⁴¹, P.G. Russek ², R. Russo ⁸⁴, A. Rustamov ⁸¹, E. Ryabinkin ¹⁴⁰, Y. Ryabov ¹⁴⁰, A. Rybicki ¹⁰⁷, H. Rytkonen ¹¹⁵, W. Rzesz ¹³³, O.A.M. Saarimaki ⁴³, R. Sadek ¹⁰⁴, S. Sadhu ³¹, S. Sadovsky ¹⁴⁰, J. Saetre ²⁰, K. Šafařík ³⁵, S. Saha ⁸⁰, B. Sahoo ⁴⁶, R. Sahoo ⁴⁷, S. Sahoo ⁶⁰, D. Sahu ⁴⁷, P.K. Sahu ⁶⁰, J. Saini ¹³², K. Sajdakova ³⁷, S. Sakai ¹²³, M.P. Salvan ⁹⁸, S. Sambyal ⁹¹, T.B. Saramela ¹¹⁰, D. Sarkar ¹³⁴, N. Sarkar ¹³², P. Sarma ⁴¹, V. Sarritzu ²², V.M. Sarti ⁹⁶, M.H.P. Sas ¹³⁷, J. Schambach ⁸⁷, H.S. Scheid ⁶³, C. Schiaua ⁴⁵, R. Schicker ⁹⁵, A. Schmah ⁹⁵, C. Schmidt ⁹⁸, H.R. Schmidt ⁹⁴, M.O. Schmidt ³², M. Schmidt ⁹⁴, N.V. Schmidt ⁸⁷, A.R. Schmier ¹²⁰, R. Schotter ¹²⁷, J. Schukraft ³², K. Schwarz ⁹⁸, K. Schweda ⁹⁸, G. Scioli ²⁵, E. Scomparin ⁵⁵, J.E. Seger ¹⁴, Y. Sekiguchi ¹²², D. Sekihata ¹²², I. Selyuzhenkov ^{98,140}, S. Senyukov ¹²⁷, J.J. Seo ⁵⁷, D. Serebryakov ¹⁴⁰, L. Šerkšnytė ⁹⁶, A. Sevcenco ⁶², T.J. Shaba ⁶⁷, A. Shabetai ¹⁰⁴, R. Shahoyan ³², A. Shangaraev ¹⁴⁰, A. Sharma ⁹⁰, D. Sharma ⁴⁶, H. Sharma ¹⁰⁷, M. Sharma ⁹¹, N. Sharma ⁹⁰, S. Sharma ⁷⁶, S. Sharma ⁹¹, U. Sharma ⁹¹, A. Shatat ⁷², O. Sheibani ¹¹⁴, K. Shigaki ⁹³, M. Shimomura ⁷⁷, S. Shirinkin ¹⁴⁰, Q. Shou ³⁹, Y. Sibirskiak ¹⁴⁰, S. Siddhanta ⁵¹, T. Siemiarczuk ⁷⁹, T.F. Silva ¹¹⁰, D. Silvermyr ⁷⁵, T. Simantathammakul ¹⁰⁵, R. Simeonov ³⁶, G. Simonetti ³², B. Singh ⁹¹, B. Singh ⁹⁶, R. Singh ⁸⁰, R. Singh ⁹¹, R. Singh ⁴⁷, S. Singh ¹⁵, V.K. Singh ¹³², V. Singhal ¹³², T. Sinha ¹⁰⁰, B. Sitar ¹², M. Sitta ^{130,55}, T.B. Skaali ¹⁹, G. Skorodumovs ⁹⁵, M. Slupecki ⁴³, N. Smirnov ¹³⁷, R.J.M. Snellings ⁵⁸, E.H. Solheim ¹⁹, C. Soncco ¹⁰², J. Song ¹¹⁴, A. Songmoolnak ¹⁰⁵, F. Soramel ²⁷, S. Sorensen ¹²⁰, R. Spijkers ⁸⁴, I. Sputowska ¹⁰⁷, J. Staa ⁷⁵, J. Stachel ⁹⁵, I. Stan ⁶², P.J. Steffanic ¹²⁰, S.F. Stiefelmaier ⁹⁵, D. Stocco ¹⁰⁴, I. Storehaug ¹⁹, M.M. Storetvedt ³⁴, P. Stratmann ¹³⁵, S. Strazzi ²⁵, C.P. Stylianidis ⁸⁴, A.A.P. Suaide ¹¹⁰, C. Suire ⁷², M. Sukhanov ¹⁴⁰, M. Suljic ³², V. Sumberia ⁹¹, S. Sumowidagdo ⁸², S. Swain ⁶⁰, I. Szarka ¹², U. Tabassam ¹³, S.F. Taghavi ⁹⁶, G. Taillepied ⁹⁸, J. Takahashi ¹¹¹, G.J. Tambave ²⁰, S. Tang ^{125,6}, Z. Tang ¹¹⁸, J.D. Tapia Takaki ¹¹⁶, N. Tapus ¹²⁴, L.A. Tarasovicova ¹³⁵, M.G. Tarzila ⁴⁵, G.F. Tassielli ³¹, A. Tauro ³², A. Telesca ³², L. Terlizzi ²⁴, C. Terrevoli ¹¹⁴, G. Tersimonov ³, D. Thomas ¹⁰⁸, A. Tikhonov ¹⁴⁰, A.R. Timmins ¹¹⁴, M. Tkacik ¹⁰⁶, T. Tkacik ¹⁰⁶, A. Toia ⁶³, R. Tokumoto ⁹³, N. Topilskaya ¹⁴⁰, M. Toppi ⁴⁸, F. Torales-Acosta ¹⁸, T. Tork ⁷², A.G. Torres Ramos ³¹, A. Trifiró ^{30,52}, A.S. Triolo ^{30,52}, S. Tripathy ⁵⁰, T. Tripathy ⁴⁶, S. Trogolo ³², V. Trubnikov ³, W.H. Trzaska ¹¹⁵, T.P. Trzciński ¹³³, R. Turrisi ⁵³, T.S. Tveter ¹⁹, K. Ullaland ²⁰, B. Ulukutlu ⁹⁶, A. Uras ¹²⁶, M. Urioni ^{54,131}, G.L. Usai ²², M. Vala ³⁷, N. Valle ²¹, S. Vallero ⁵⁵, L.V.R. van Doremalen ⁵⁸, M. van Leeuwen ⁸⁴, C.A. van Veen ⁹⁵, R.J.G. van Weelden ⁸⁴, P. Vande Vyvre ³², D. Varga ¹³⁶, Z. Varga ¹³⁶, M. Varga-Kofarago ¹³⁶, M. Vasileiou ⁷⁸, A. Vasiliev ¹⁴⁰, O. Vázquez Doce ⁹⁶, V. Vechernin ¹⁴⁰, E. Vercellin ²⁴, S. Vergara Limón ⁴⁴, L. Vermunt ⁹⁸, R. Vértesi ¹³⁶, M. Verweij ⁵⁸, L. Vickovic ³³, Z. Vilakazi ¹²¹, O. Villalobos Baillie ¹⁰¹, G. Vino ⁴⁹, A. Vinogradov ¹⁴⁰, T. Virgili ²⁸, V. Vislavicius ⁸³, A. Vodopyanov ¹⁴¹, B. Volkel ³², M.A. Völk ⁹⁵, K. Voloshin ¹⁴⁰, S.A. Voloshin ¹³⁴, G. Volpe ³¹, B. von Haller ³², I. Vorobyev ⁹⁶, N. Vozniuk ¹⁴⁰, J. Vrláková ³⁷, B. Wagner ²⁰, C. Wang ³⁹, D. Wang ³⁹, M. Weber ¹⁰³, A. Wegrzynek ³², F.T. Weiglhofer ³⁸, S.C. Wenzel ³², J.P. Wessels ¹³⁵, S.L. Weyhmiller ¹³⁷, J. Wiechula ⁶³, J. Wikne ¹⁹, G. Wilk ⁷⁹, J. Wilkinson ⁹⁸, G.A. Willems ¹³⁵, B. Windelband ⁹⁵, M. Winn ¹²⁸, J.R. Wright ¹⁰⁸, W. Wu ³⁹, Y. Wu ¹¹⁸, R. Xu ⁶, A. Yadav ⁴², A.K. Yadav ¹³², S. Yalcin ⁷¹, Y. Yamaguchi ⁹³, K. Yamakawa ⁹³, S. Yang ²⁰, S. Yano ⁹³, Z. Yin ⁶, I.-K. Yoo ¹⁶, J.H. Yoon ⁵⁷, S. Yuan ²⁰, A. Yuncu ⁹⁵, V. Zaccolo ²³,

C. Zampolli ³², H.J.C. Zanolli⁵⁸, F. Zanone ⁹⁵, N. Zardoshti ^{32,101}, A. Zarochentsev ¹⁴⁰, P. Závada ⁶¹, N. Zaviyalov¹⁴⁰, M. Zhalov ¹⁴⁰, B. Zhang ⁶, S. Zhang ³⁹, X. Zhang ⁶, Y. Zhang¹¹⁸, Z. Zhang ⁶, M. Zhao ¹⁰, V. Zherebchevskii ¹⁴⁰, Y. Zhi¹⁰, N. Zhigareva¹⁴⁰, D. Zhou ⁶, Y. Zhou ⁸³, J. Zhu ^{98,6}, Y. Zhu⁶, G. Zinovjev^{1,3}, N. Zurlo ^{131,54}

Affiliation Notes

^I Deceased

^{II} Also at: Max-Planck-Institut für Physik, Munich, Germany

^{III} Also at: Italian National Agency for New Technologies, Energy and Sustainable Economic Development (ENEA), Bologna, Italy

^{IV} Also at: Dipartimento DET del Politecnico di Torino, Turin, Italy

^V Also at: Department of Applied Physics, Aligarh Muslim University, Aligarh, India

^{VI} Also at: Institute of Theoretical Physics, University of Wroclaw, Poland

^{VII} Also at: An institution covered by a cooperation agreement with CERN

Collaboration Institutes

¹ A.I. Alikhanyan National Science Laboratory (Yerevan Physics Institute) Foundation, Yerevan, Armenia

² AGH University of Science and Technology, Cracow, Poland

³ Bogolyubov Institute for Theoretical Physics, National Academy of Sciences of Ukraine, Kiev, Ukraine

⁴ Bose Institute, Department of Physics and Centre for Astroparticle Physics and Space Science (CAPSS), Kolkata, India

⁵ California Polytechnic State University, San Luis Obispo, California, United States

⁶ Central China Normal University, Wuhan, China

⁷ Centro de Aplicaciones Tecnológicas y Desarrollo Nuclear (CEADEN), Havana, Cuba

⁸ Centro de Investigación y de Estudios Avanzados (CINVESTAV), Mexico City and Mérida, Mexico

⁹ Chicago State University, Chicago, Illinois, United States

¹⁰ China Institute of Atomic Energy, Beijing, China

¹¹ Chungbuk National University, Cheongju, Republic of Korea

¹² Comenius University Bratislava, Faculty of Mathematics, Physics and Informatics, Bratislava, Slovak Republic

¹³ COMSATS University Islamabad, Islamabad, Pakistan

¹⁴ Creighton University, Omaha, Nebraska, United States

¹⁵ Department of Physics, Aligarh Muslim University, Aligarh, India

¹⁶ Department of Physics, Pusan National University, Pusan, Republic of Korea

¹⁷ Department of Physics, Sejong University, Seoul, Republic of Korea

¹⁸ Department of Physics, University of California, Berkeley, California, United States

¹⁹ Department of Physics, University of Oslo, Oslo, Norway

²⁰ Department of Physics and Technology, University of Bergen, Bergen, Norway

²¹ Dipartimento di Fisica, Università di Pavia, Pavia, Italy

²² Dipartimento di Fisica dell’Università and Sezione INFN, Cagliari, Italy

²³ Dipartimento di Fisica dell’Università and Sezione INFN, Trieste, Italy

²⁴ Dipartimento di Fisica dell’Università and Sezione INFN, Turin, Italy

²⁵ Dipartimento di Fisica e Astronomia dell’Università and Sezione INFN, Bologna, Italy

²⁶ Dipartimento di Fisica e Astronomia dell’Università and Sezione INFN, Catania, Italy

²⁷ Dipartimento di Fisica e Astronomia dell’Università and Sezione INFN, Padova, Italy

²⁸ Dipartimento di Fisica ‘E.R. Caianiello’ dell’Università and Gruppo Collegato INFN, Salerno, Italy

²⁹ Dipartimento DISAT del Politecnico and Sezione INFN, Turin, Italy

³⁰ Dipartimento di Scienze MIFT, Università di Messina, Messina, Italy

³¹ Dipartimento Interateneo di Fisica ‘M. Merlin’ and Sezione INFN, Bari, Italy

³² European Organization for Nuclear Research (CERN), Geneva, Switzerland

³³ Faculty of Electrical Engineering, Mechanical Engineering and Naval Architecture, University of Split, Split, Croatia

³⁴ Faculty of Engineering and Science, Western Norway University of Applied Sciences, Bergen, Norway

³⁵ Faculty of Nuclear Sciences and Physical Engineering, Czech Technical University in Prague, Prague, Czech Republic

- ³⁶ Faculty of Physics, Sofia University, Sofia, Bulgaria
³⁷ Faculty of Science, P.J. Šafárik University, Košice, Slovak Republic
³⁸ Frankfurt Institute for Advanced Studies, Johann Wolfgang Goethe-Universität Frankfurt, Frankfurt, Germany
³⁹ Fudan University, Shanghai, China
⁴⁰ Gangneung-Wonju National University, Gangneung, Republic of Korea
⁴¹ Gauhati University, Department of Physics, Guwahati, India
⁴² Helmholtz-Institut für Strahlen- und Kernphysik, Rheinische Friedrich-Wilhelms-Universität Bonn, Bonn, Germany
⁴³ Helsinki Institute of Physics (HIP), Helsinki, Finland
⁴⁴ High Energy Physics Group, Universidad Autónoma de Puebla, Puebla, Mexico
⁴⁵ Horia Hulubei National Institute of Physics and Nuclear Engineering, Bucharest, Romania
⁴⁶ Indian Institute of Technology Bombay (IIT), Mumbai, India
⁴⁷ Indian Institute of Technology Indore, Indore, India
⁴⁸ INFN, Laboratori Nazionali di Frascati, Frascati, Italy
⁴⁹ INFN, Sezione di Bari, Bari, Italy
⁵⁰ INFN, Sezione di Bologna, Bologna, Italy
⁵¹ INFN, Sezione di Cagliari, Cagliari, Italy
⁵² INFN, Sezione di Catania, Catania, Italy
⁵³ INFN, Sezione di Padova, Padova, Italy
⁵⁴ INFN, Sezione di Pavia, Pavia, Italy
⁵⁵ INFN, Sezione di Torino, Turin, Italy
⁵⁶ INFN, Sezione di Trieste, Trieste, Italy
⁵⁷ Inha University, Incheon, Republic of Korea
⁵⁸ Institute for Gravitational and Subatomic Physics (GRASP), Utrecht University/Nikhef, Utrecht, Netherlands
⁵⁹ Institute of Experimental Physics, Slovak Academy of Sciences, Košice, Slovak Republic
⁶⁰ Institute of Physics, Homi Bhabha National Institute, Bhubaneswar, India
⁶¹ Institute of Physics of the Czech Academy of Sciences, Prague, Czech Republic
⁶² Institute of Space Science (ISS), Bucharest, Romania
⁶³ Institut für Kernphysik, Johann Wolfgang Goethe-Universität Frankfurt, Frankfurt, Germany
⁶⁴ Instituto de Ciencias Nucleares, Universidad Nacional Autónoma de México, Mexico City, Mexico
⁶⁵ Instituto de Física, Universidade Federal do Rio Grande do Sul (UFRGS), Porto Alegre, Brazil
⁶⁶ Instituto de Física, Universidad Nacional Autónoma de México, Mexico City, Mexico
⁶⁷ iThemba LABS, National Research Foundation, Somerset West, South Africa
⁶⁸ Jeonbuk National University, Jeonju, Republic of Korea
⁶⁹ Johann-Wolfgang-Goethe Universität Frankfurt Institut für Informatik, Fachbereich Informatik und Mathematik, Frankfurt, Germany
⁷⁰ Korea Institute of Science and Technology Information, Daejeon, Republic of Korea
⁷¹ KTO Karatay University, Konya, Turkey
⁷² Laboratoire de Physique des 2 Infinis, Irène Joliot-Curie, Orsay, France
⁷³ Laboratoire de Physique Subatomique et de Cosmologie, Université Grenoble-Alpes, CNRS-IN2P3, Grenoble, France
⁷⁴ Lawrence Berkeley National Laboratory, Berkeley, California, United States
⁷⁵ Lund University Department of Physics, Division of Particle Physics, Lund, Sweden
⁷⁶ Nagasaki Institute of Applied Science, Nagasaki, Japan
⁷⁷ Nara Women's University (NWU), Nara, Japan
⁷⁸ National and Kapodistrian University of Athens, School of Science, Department of Physics , Athens, Greece
⁷⁹ National Centre for Nuclear Research, Warsaw, Poland
⁸⁰ National Institute of Science Education and Research, Homi Bhabha National Institute, Jatni, India
⁸¹ National Nuclear Research Center, Baku, Azerbaijan
⁸² National Research and Innovation Agency - BRIN, Jakarta, Indonesia
⁸³ Niels Bohr Institute, University of Copenhagen, Copenhagen, Denmark
⁸⁴ Nikhef, National institute for subatomic physics, Amsterdam, Netherlands
⁸⁵ Nuclear Physics Group, STFC Daresbury Laboratory, Daresbury, United Kingdom
⁸⁶ Nuclear Physics Institute of the Czech Academy of Sciences, Husinec-Řež, Czech Republic
⁸⁷ Oak Ridge National Laboratory, Oak Ridge, Tennessee, United States
⁸⁸ Ohio State University, Columbus, Ohio, United States

- ⁸⁹ Physics department, Faculty of science, University of Zagreb, Zagreb, Croatia
⁹⁰ Physics Department, Panjab University, Chandigarh, India
⁹¹ Physics Department, University of Jammu, Jammu, India
⁹² Physics Department, University of Rajasthan, Jaipur, India
⁹³ Physics Program and International Institute for Sustainability with Knotted Chiral Meta Matter (SKCM2), Hiroshima University, Hiroshima, Japan
⁹⁴ Physikalisches Institut, Eberhard-Karls-Universität Tübingen, Tübingen, Germany
⁹⁵ Physikalisches Institut, Ruprecht-Karls-Universität Heidelberg, Heidelberg, Germany
⁹⁶ Physik Department, Technische Universität München, Munich, Germany
⁹⁷ Politecnico di Bari and Sezione INFN, Bari, Italy
⁹⁸ Research Division and ExtreMe Matter Institute EMMI, GSI Helmholtzzentrum für Schwerionenforschung GmbH, Darmstadt, Germany
⁹⁹ Saga University, Saga, Japan
¹⁰⁰ Saha Institute of Nuclear Physics, Homi Bhabha National Institute, Kolkata, India
¹⁰¹ School of Physics and Astronomy, University of Birmingham, Birmingham, United Kingdom
¹⁰² Sección Física, Departamento de Ciencias, Pontificia Universidad Católica del Perú, Lima, Peru
¹⁰³ Stefan Meyer Institut für Subatomare Physik (SMI), Vienna, Austria
¹⁰⁴ SUBATECH, IMT Atlantique, Nantes Université, CNRS-IN2P3, Nantes, France
¹⁰⁵ Suranaree University of Technology, Nakhon Ratchasima, Thailand
¹⁰⁶ Technical University of Košice, Košice, Slovak Republic
¹⁰⁷ The Henryk Niewodniczanski Institute of Nuclear Physics, Polish Academy of Sciences, Cracow, Poland
¹⁰⁸ The University of Texas at Austin, Austin, Texas, United States
¹⁰⁹ Universidad Autónoma de Sinaloa, Culiacán, Mexico
¹¹⁰ Universidade de São Paulo (USP), São Paulo, Brazil
¹¹¹ Universidade Estadual de Campinas (UNICAMP), Campinas, Brazil
¹¹² Universidade Federal do ABC, Santo Andre, Brazil
¹¹³ University of Cape Town, Cape Town, South Africa
¹¹⁴ University of Houston, Houston, Texas, United States
¹¹⁵ University of Jyväskylä, Jyväskylä, Finland
¹¹⁶ University of Kansas, Lawrence, Kansas, United States
¹¹⁷ University of Liverpool, Liverpool, United Kingdom
¹¹⁸ University of Science and Technology of China, Hefei, China
¹¹⁹ University of South-Eastern Norway, Kongsberg, Norway
¹²⁰ University of Tennessee, Knoxville, Tennessee, United States
¹²¹ University of the Witwatersrand, Johannesburg, South Africa
¹²² University of Tokyo, Tokyo, Japan
¹²³ University of Tsukuba, Tsukuba, Japan
¹²⁴ University Politehnica of Bucharest, Bucharest, Romania
¹²⁵ Université Clermont Auvergne, CNRS/IN2P3, LPC, Clermont-Ferrand, France
¹²⁶ Université de Lyon, CNRS/IN2P3, Institut de Physique des 2 Infinis de Lyon, Lyon, France
¹²⁷ Université de Strasbourg, CNRS, IPHC UMR 7178, F-67000 Strasbourg, France, Strasbourg, France
¹²⁸ Université Paris-Saclay Centre d'Etudes de Saclay (CEA), IRFU, Département de Physique Nucléaire (DPhN), Saclay, France
¹²⁹ Università degli Studi di Foggia, Foggia, Italy
¹³⁰ Università del Piemonte Orientale, Vercelli, Italy
¹³¹ Università di Brescia, Brescia, Italy
¹³² Variable Energy Cyclotron Centre, Homi Bhabha National Institute, Kolkata, India
¹³³ Warsaw University of Technology, Warsaw, Poland
¹³⁴ Wayne State University, Detroit, Michigan, United States
¹³⁵ Westfälische Wilhelms-Universität Münster, Institut für Kernphysik, Münster, Germany
¹³⁶ Wigner Research Centre for Physics, Budapest, Hungary
¹³⁷ Yale University, New Haven, Connecticut, United States
¹³⁸ Yonsei University, Seoul, Republic of Korea
¹³⁹ Zentrum für Technologie und Transfer (ZTT), Worms, Germany
¹⁴⁰ Affiliated with an institute covered by a cooperation agreement with CERN
¹⁴¹ Affiliated with an international laboratory covered by a cooperation agreement with CERN.